NASA CR–189088
January 1992

NASA

National Aeronautics and
Space Administration

Contract NAS3–23687

COMPONENT-SPECIFIC MODELING

FINAL REPORT

By

R.L McKnight
R.J. Maffeo
M.T. Tipton
G. Weber

General Electric Company
Aircraft Engines
Cincinnati, Ohio 45215

Prepared For
National Aeronautics and Space Administration
Lewis Research Center
21000 Brookpark Road
Cleveland, Ohio 44135

NASA

National Aeronautics and
Space Administration

Contract NAS3–23687

COMPONENT-SPECIFIC MODELING

FINAL REPORT

Foreword

This report has been prepared to expedite early domestic dissemination of the information generated under the contract. The NASA program manager is Dr. M.S. Hirschbein.

Abstract

Accomplishments are described for a 3-year program to develop methodology for component-specific modeling of aircraft engine hot section components (turbine blades, turbine vanes, and burner liners). These accomplishments include: (1) engine thermodynamic and mission models, (2) geometry model generators, (3) remeshing, (4) specialty 3D inelastic structural analysis, (5) computationally efficient solvers, (6) adaptive solution strategies, (7) engine performance parameters/component response variables decomposition and synthesis, (8) integrated software architecture and development, and (9) validation cases for software developed.

GE Aircraft Engines

General Electric Company
P.O. Box 156301, One Neumann Way
Cincinnati, OH 45215-6301
513 243 2000

March 2, 1992

SUBJECT: CONTRACT NAS3-23687
COMPONENT-SPECIFIC MODELING
FINAL/FINAL REPORT

TO: National Aeronautics and
Space Administration
Lewis Research Center
21000 Brookpark Road
Cleveland, OH 44135

ATTN: Christos Chamis, MS 49-6

Submitted herewith are three copies of the final/final report per contract requirements.

Additional distribution is being made in accordance with the distribution list provided by NASA.

This completes all contract requirements per NASA letter dated November 21, 1991 and discussions with C. Chamis.

Very truly yours,

GE AIRCRAFT ENGINES

Jeanette Sturgill

J. M. Sturgill
Program Management Specialist
(513) 774-4280

cc: (letter only)
NASA Contracting Officer, MS 500-312 (R. A. Erten)
DPRO/PDO N-1
DPRO/TMD N-1
Contracts A306
C. Cash, Cleveland Office
File

TABLE OF CONTENTS

TABLE OF CONTENTS
(continued)

LIST OF ILLUSTRATIONS

LIST OF TABLES

NOMENCLATURE

C_c = Bound on creep strain gradient

C_p = Bound on plastic strain gradient

C_R = Maximum allowable sum of R_i

C_{RiL} = Lower bound for R_i for possible remeshing

C_{Riu} = Maximum allowable upper bound for R_i

C_s = Bound separating remeshing from re-solving

E^A = Absolute error in vector norms

E^R = Relative error in vector norms

$\{F\}$ = Vector of external forces in FEM analysis

h_c = Convection heat transfer coefficient $\frac{\text{Btu}}{\text{hr-ft}^2\text{-}^\circ\text{F}}$

h_r = Equivalent heat transfer coefficient for radiation to casing $\frac{\text{Btu}}{\text{hr-ft}^2\text{-}^\circ\text{F}}$

K = Metal conductivity, $\frac{\text{Btu}}{\text{ft}^2\text{-hr-}^\circ\text{F}}$

$[K]$ = Stiffness matrix for FEM analysis

P_3 = Compressor discharge total pressure, psia

Q/A = Heat flux through material, $\frac{\text{Btu}}{\text{hr-ft}^2}$

$\{R\}$ = Vector of residual forces in FEM analysis

R_i = i^{th} residual force

THTD = General Electric proprietary 3D transient heat transfer analysis computer program

TOL = Tolerance on local integration error

T_H = Hot side metal temperature, °F

T_c = Cold side metal temperature, °F

T_{LINER} = Bulk liner temperature, °F

T_3 = Compressor discharge temperature, °F

T_4 = HP turbine rotor inlet temperature, °F

T_{41} = HP turbine inlet gas temperature, °F

T_{ij} = Temperature at position ij, °F

T_{mij} = Combustor metal temperature at position ij, °F

t = Material thickness, Pt

Δt_i = Current time subincrement

Δt_{i+1} = Next time subincrement

W_{41} = Turbine airflow, #/sec

11X11 = Vector norm

YC = Cooling effectiveness, dimensionless

k, n, m, q, r = Temperature dependent material creep parameters

{S} = Vector of displacements in FEM analysis

$(\Delta S_e)_{allowable}$ = Maximum allowable stress change

$(\Delta S_e)_{max}$ = Maximum change in stress occurring in the current time step.

E_c = Creep strain, m/m

E_p = Plastic strain, in/in

E_i = Total strain at point i, in/in

E_i^c = Creep strain at point i, in/in

E_i^e = Elastic strain at point i, in/in

E_i^P = Plastic strain at point i, in/in

E_i^t = Thermal strain at point i, in/in

$\ddot{E}^I$ = Second derivative of the inelastic strain rate

$(\Delta E_e^I)_{allowable}$ = Maximum allowable inelastic strain increment

$(\Delta E_e^I)_{max}$ = Maximum inelastic strain increment occurring in the current time step

N_c = Nominal cooling effectiveness, dimensionless

N_{cs} = Cooling effectiveness at specified span, dimensionless

N_{cms} = Cooling effectiveness at midspan, dimensionless

1.0 INTRODUCTION

Modern jet engine design imposes extremely high loadings and temperatures on hot section components. Fuel costs dictate that minimum weight components be used wherever possible. In order to satisfy these two criteria, designers are turning toward improved materials and innovative designs. Along with these approaches, they also must have more accurate, more economical, and more comprehensive analytical methods.

Numerous analytical methods are available that can, in principle, handle any problem that might arise. However, the time and expense required to produce acceptable solutions is often excessive. This program addresses this problem by setting out a plan to create specialized software packages which will provide the necessary answers in an efficient, user-oriented, streamlined fashion. Separate component-specific models will be created for burner liners, turbine blades, and turbine vanes using fundamental data from many technical areas. The methods developed will be simple to execute, but they will not be simple in concept. The problem is extremely complex and only by a thorough understanding of the details can the important technical approaches be extracted. The packaging of these interdisciplinary approaches into a total system must conform to the modular requirements for useful computer programs.

The overall objective of this program was to develop and verify a series of interdisciplinary modeling and analysis techniques that have been specialized to address three specific hot section components. These techniques incorporate data as well as theoretical methods from many diverse areas including cycle and performance analysis, heat transfer analysis, linear and nonlinear stress analysis, and mission analysis. Building on the proven techniques already available in these fields, the new methods developed through this contract have been integrated to provide an accurate, efficient, and unified approach to analyzing combustor burner liners, hollow air-cooled turbine blades, and air-cooled turbine vanes. For these components, the methods developed predict temperature, deformation, stress, and strain histories throughout a complete flight mission.

This program, to a great extent, drew on prior experience. This base of experience was invaluable for understanding the highly complex intersections among all the different technical disciplines as well as for estimating the importance of different engine parameters. In particular, there are four specific areas in which experience was especially beneficial.

First, with the recent increases in fuel costs, greater emphasis has been placed on more accurate solutions for stresses and strains in order to understand and improve the durability and life of hot section components; conventional linear elastic analyses are no longer sufficient; instead, they now provide the boundary values for more refined creep and plasticity calculations. These nonlinear analyses are now performed routinely as part of the design process at General Electric. This extensive experience with these plasticity and creep methods contributed directly to developing component specific models.

Second, advances in 3-D modeling capability are being achieved by the concepts developed under the NASA-supported ESMOSS program. ESMOSS concepts provided the basis to develop an efficient modeling system for geometric and discretized models of engine components.

Third, the NASA-funded Burner Liner Thermal/Structural Load Modeling Program contributed strong support to this program. The specific area addressed the transfer of data from a 3-D heat transfer analysis model to a 3-D stress analysis model and provided the background and framework for the data interpolation required for all thermomechanical models in this contract.

Fourth, over the past 10 years General Electric has developed internally a family of computer programs: LASTS, OPSEV, and HOTSAM. These programs all have the common thread of using selected points from cycle data, heat transfer and stress analyses, and a decomposition/synthesis approach to produce accurate values of temperature, stress, and strain throughout a mission. These programs were totally consistent with the overall objectives of this program and represented a proven technology base upon which the component specific models were developed. Significant advances were made in the inclusion of nonlinear effects and the introduction of improved modeling and data transfer techniques.

The program was organized into nine tasks which were logically separated into two broadly parallel activities (Figure 1). On the right of Figure 1 is the Component Specific Thermomechanical Load Mission Modeling path. Along this path a Decomposition/Synthesis approach was taken. In broad terms, methods were developed to generate approximate numerical models for the engine cycle and the aerodynamic and heat transfer analyses needed to provide the input conditions for hot parts stress and life analysis.

The left path, Component Specific Structural Modeling, provided the tools to develop and analyze finite element nonlinear stress analysis models of combustor liners, turbine blades, and vanes. These two paths are shown in more detail in Figures 2 and 3.

Software Development, Task IV, consisted of planning and writing the computer programs for both paths, with the necessary interconnections, using a structured, top down approach.

In the Thermomechanical Load Mission Modeling portion of the program (Task III), a Thermodynamic Engine Model was developed which generates the engine internal flow variables for any point on the operating mission. Figure 2 diagrams the tasks. The method for doing this is described below. Task V was developing techniques to decompose flight missions into characteristic mission segments. In Task VII a Thermomechanical Mission Model was developed. This uses the flow variables from the Thermodynamic Model to determine metal temperature and pressure distributions for a representative combustor liner and turbine blade and vane.

Individual tasks for the Structural Modeling activity are shown in Figure 3. The requirements of Software Design, Task II, were factored into Task VI, the evaluation of the structural analysis methods which were selected for evaluation in Task I. Task VIII provides the capability for structurally modeling current state-of-the-art combustor liners and hollow turbine blades and vans, given the defining dimensional parameters. These parameters were chosen to facilitate parametric studies.

The component specific models were developed in two steps. In the first a geometric model is defined. In the application of the Component Specific Modeling Program these data are then transferred to the Thermomechanical Load Mission Model to provide the geometry for determining component pressures and temperatures. Thus, a data transfer link was developed to do this in Task IV, Software Development. The capability for generating from the geometric model a discretized, finite element model was a part of Task VIII. At this point another link between the two paths was needed to transfer the component temperatures and pressures from the Thermomechanical Load Model to the finite element model, interpolating the data as needed to define nodal temperatures and pressures. This was completed in Task IV.

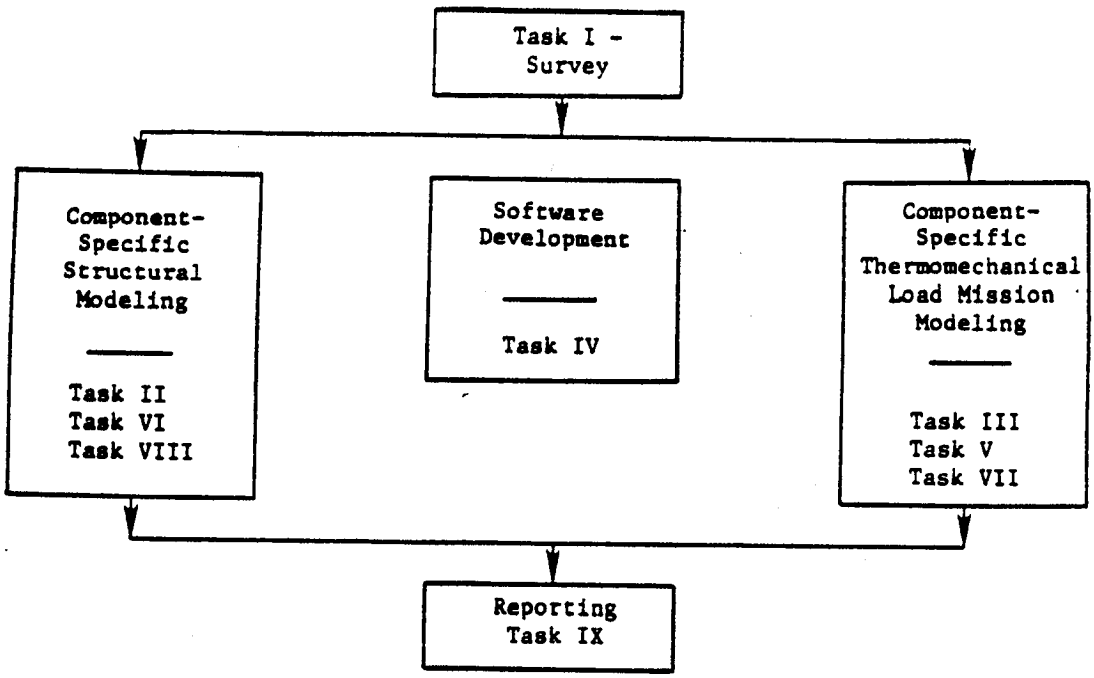

Figure 1. Component Specific Modeling Base Program.

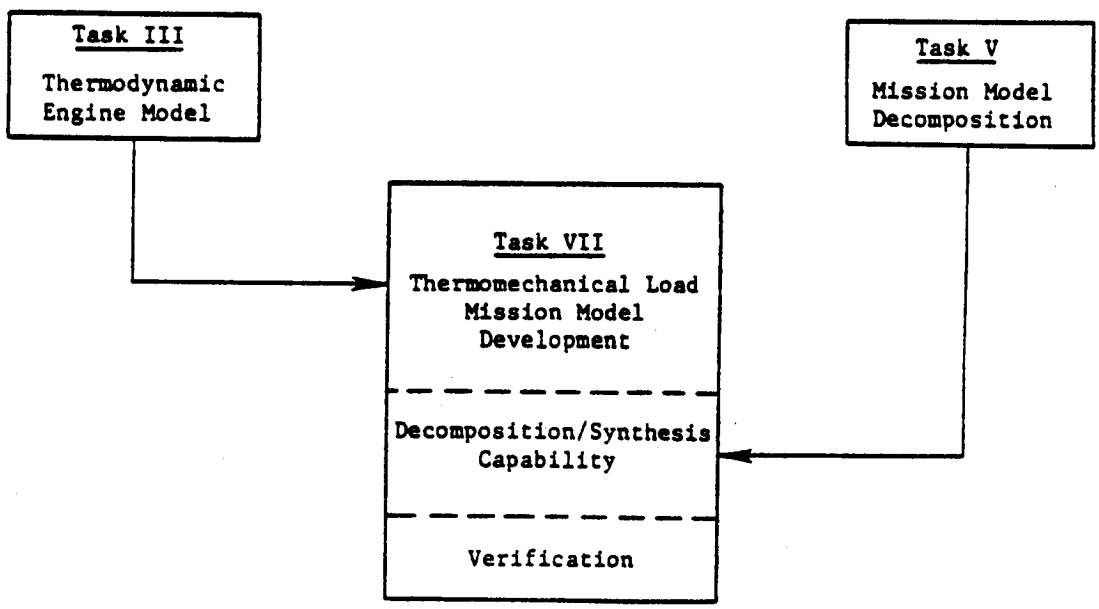

Figure 2. Component Specific Thermomechanical Load Mission Modeling.

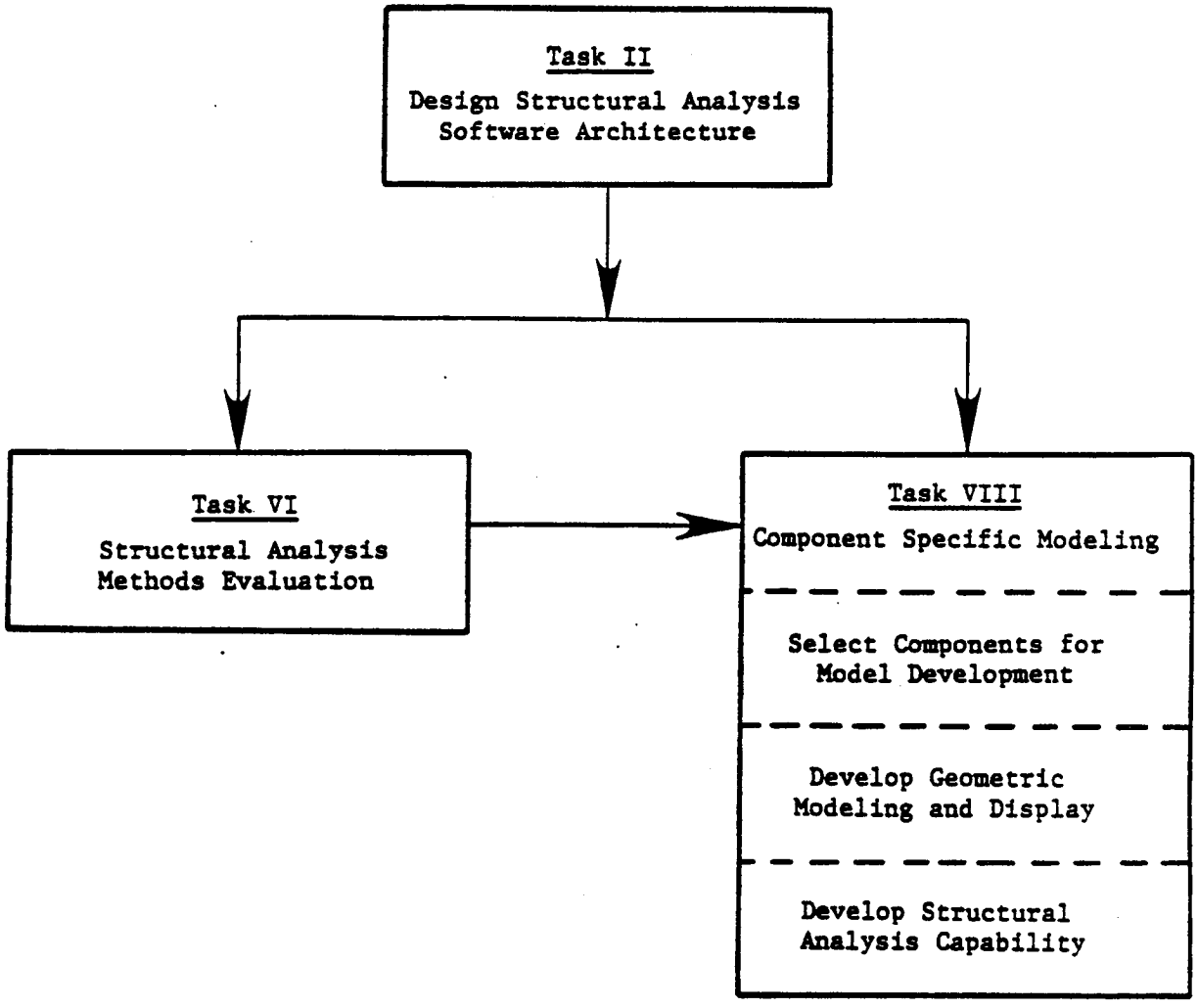

Figure 3. Component Specific Structural Modeling.

2.0 TECHNICAL PROGRESS

2.1 TASK I - LITERATURE SURVEY

The first task of this program was to perform a literature survey of available methods, techniques, and solution strategies that could be used to geometrically model, display, and structurally analyze burner liner, turbine blades and vanes. NTIS, NASA, DTIC, and internal General Electric Company documents were searched. As a result of this survey, 85 papers and 8 books and procedures were discovered with pertinent information. As a result of evaluating this information, recommendations were made on the technology to be incorporated into the program and approved by the NASA Program Manager.

2.2 TASK II - DESIGN OF STRUCTURAL ANALYSIS SOFTWARE ARCHITECTURE

The software architecture was designed using the methodology developed for the ESMOSS program. This development was carried out by a team whose members provided expertise in all of the pertinent areas. The architecture approved by the NASA Program Manager is contained in Appendix A. In addition to the program architecture, the preprocessor and postprocessor attributes are defined.

2.3 TASK III - THERMODYNAMIC ENGINE MODEL

The Thermodynamic Engine Model has been developed as a simple calculation tool which will take as inputs the three variables altitude (h), Mach number (M), and power level (PL) over the allowed flight map of an engine, as shown in Figure 4. In addition, ambient temperature deviations from the standard atmosphere, airframe bleed air requirements, and engine deterioration can also be included as part of the input to the thermodynamic model. For each input condition specified by h, M, and PL, the thermodynamic model will calculate gas weight flow ($\dot{w}$), temperature (t), and pressure (p) at selected aerodynamic engine stations as needed to determine component thermal loadings. These stations are shown in Figure 5.

The technique for developing a thermodynamic engine model is shown in Figures 6 and 7. The engine to be analyzed must be defined thermodynamically by an engine cycle deck (computer program) that can be run to generate the internal flow variables at the chosen aerodynamic stations (Figure 6). To encompass the complete engine operating map (Figure 4), 148 operating points are chosen and $\dot{w}$, t, and p are calculated using the cycle deck for the selected stations as well as N_1 and N_2, the fan and core speeds. From this station data, an engine performance cycle map is constructed. This is essentially a set of three-dimensional data arrays that map the station data ($\dot{w}$, t, p, N_1, and N_2) onto the engine operating map (Figure 4). Given an arbitrary operating point defined by h, M, and PL, it is then possible in principle to interpolate on the engine performance cycle map to determine station data. In practice the station parameters are nonlinear functions of the input parameters, and considerable effort is needed to develop these multidimensional interpolations. The computer programs used to generate the engine performance cycle map from the engine cycle deck output has been developed as part of Task III. The functioning of the thermodynamic engine model is shown in Figure 7. Given an engine mission, as shown schematically in Figure 8, it can be defined by values of the input variables h, M, and PL at selected times through the mission. Using these input variables and the engine performance cycle map, an interpolation program developed in this effort calculates engine station parameters throughout the mission (Figure 7). These are then used to define station mission profiles of $\dot{w}$, t, p, N_1, and N_2 as functions of time at each aerodynamic station. These station mission profiles then become the input to the thermomechanical engine model.

2.3.1 Detailed Specification and Requirements

The first step in this task was to develop detailed specifications and requirements for the thermodynamic engine model software. This specification, which was approved by the NASA Program Manager, is presented in Appendix C.

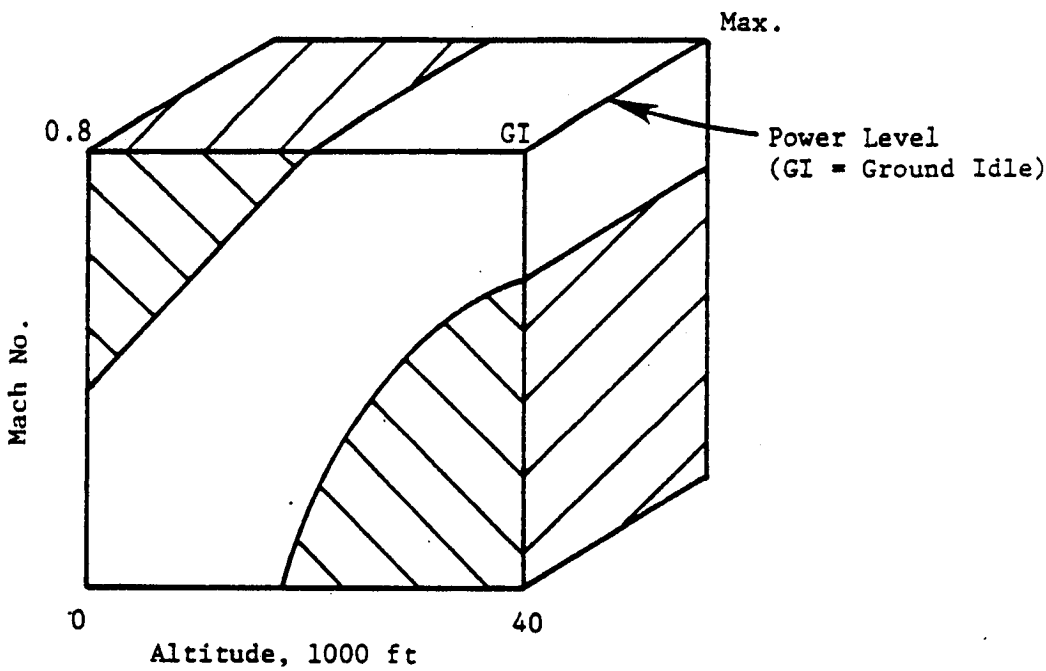

Figure 4. Engine Operating Map.

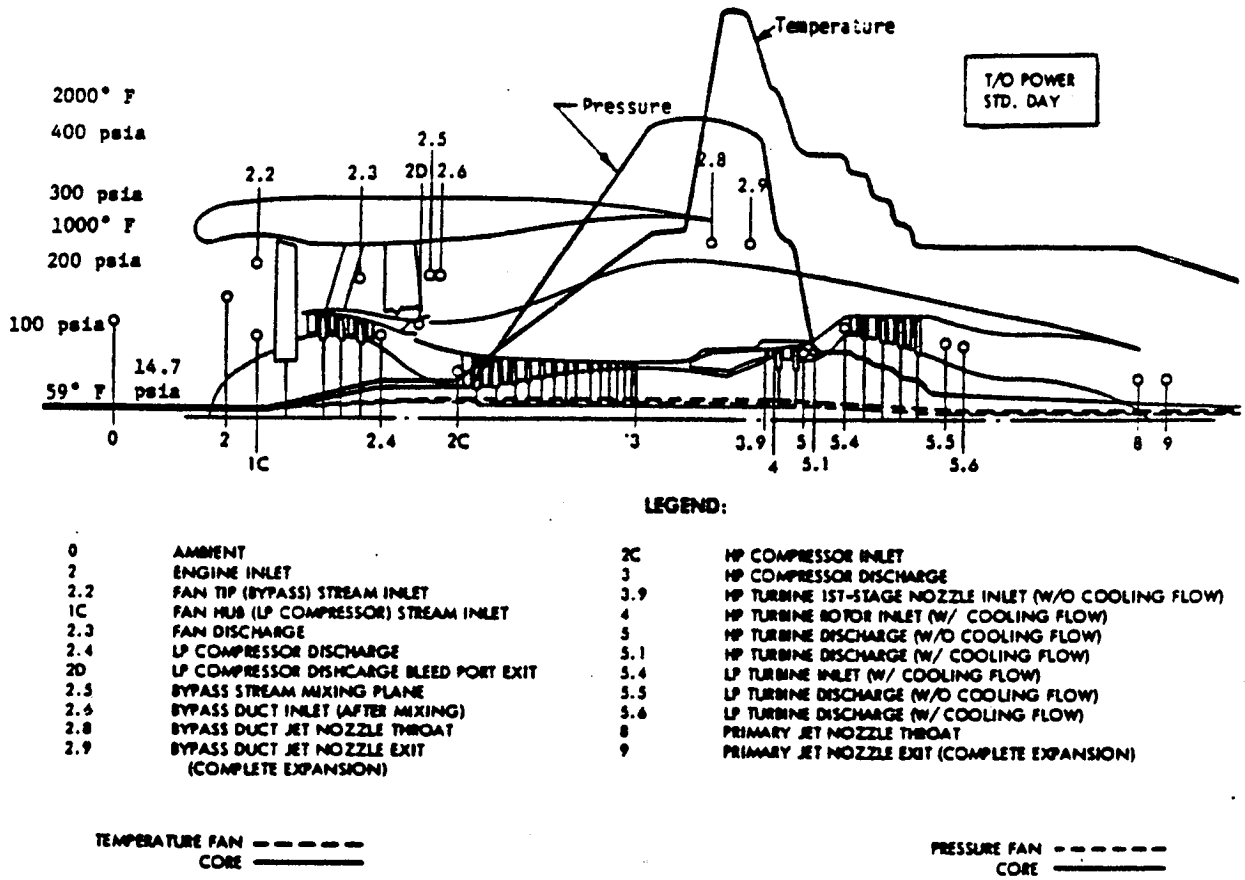

Figure 5. CF6 Aerodynamic Stations.

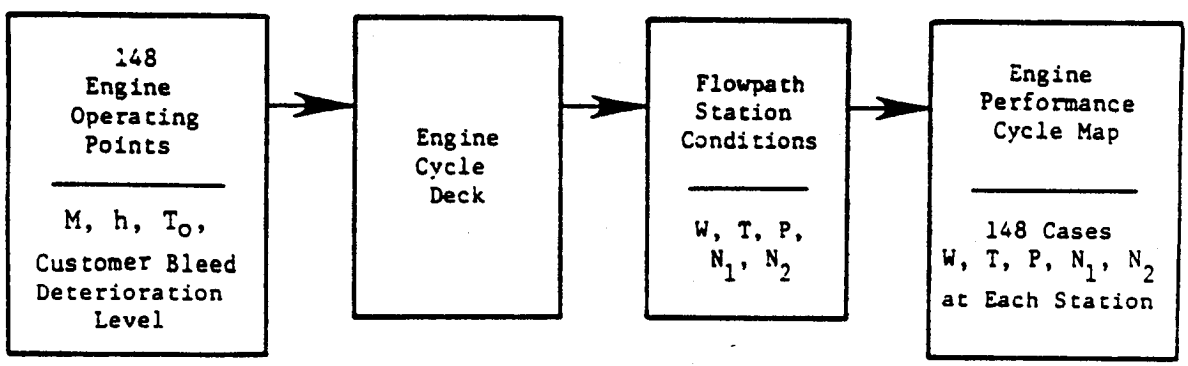

Figure 6. Thermodynamic Engine Model Cycle Map Generation.

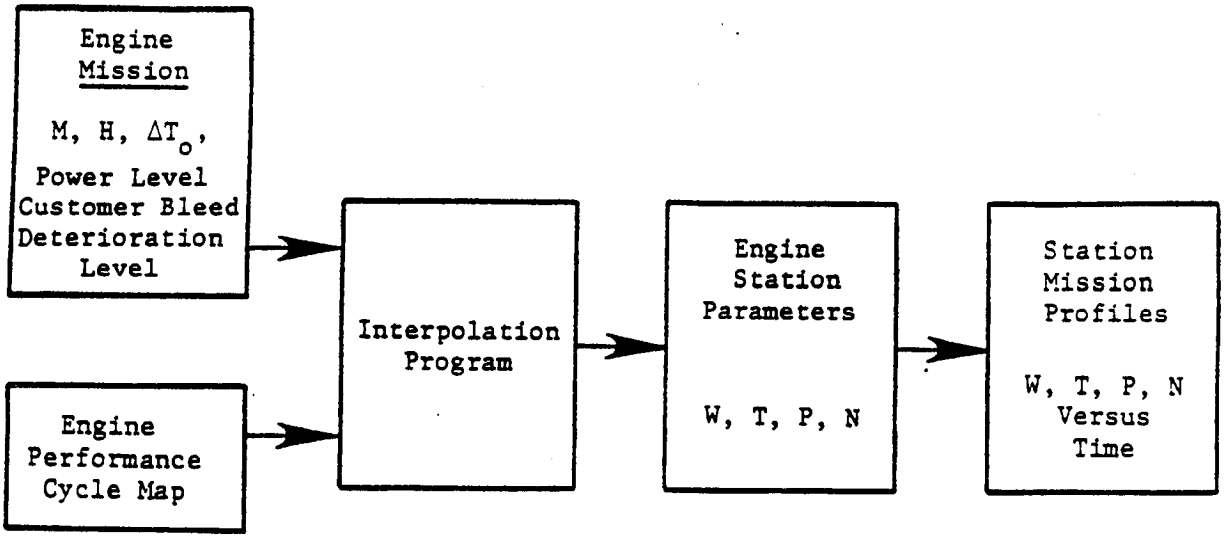

Figure 7. Thermodynamic Engine Model.

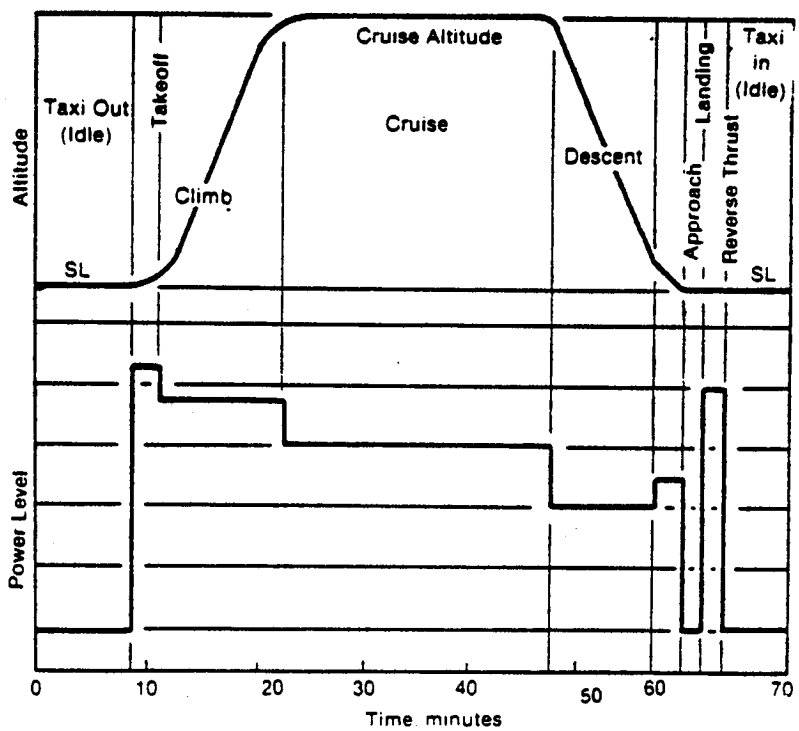

Figure 8. Typical Flight Cycle.

2.3.2 Model Design and Development

Based on the detailed specifications, the thermodynamic engine model software was generated and a set of 148 performance cases was obtained to load this model. The next task was to establish interparameter interpolation functions. To assist in this effort, 103 special cases that would maximize interpolation errors were chosen from the cycle deck.

A master interparameter linearity study was executed to evaluate interpolation functions. A computer program (STATPAC) was available that could take 30 input performance parameters, perform transformations on the data, and generate crossplots of the transformed function. The linearity of these crossplots was the criterion of excellence in the selection of interpolation functions. One hundred validation cases were run with 30 parameters each, giving 3000 individual comparisons. Sixty-three additional performance cases were used to perform the interparameter linearity study for the Mach number and altitude control variables.

Based on the above program, a set of interparameter interpolation functions and transformation functions were defined and encoded in the TDE model software. The accuracy that can be achieved with these is excellent. As a final "trial run," this model was tested against the CFM56 engine flight conditions. A TDE User's Manual has been written.

2.4 TASK IV - SOFTWARE DEVELOPMENT

2.4.1 Software System Overview

The Component Specific Modeling Program is composed of several software packages. These primary constituent software packages are the Thermodynamic Engine Model, the Thermomechanical Loads Model, the Component Specific Geometric Models, and the FEM Structural Analysis Code. Each of these software packages exist and function as separate independent codes. It has been the primary objective of the COSMOS program to concentrate the effort of

the diverse technologies into a single software system. Reference to the system design of Figure 9 provides the reader a good overview as to the structure of the COSMOS software system.

In brief, a main executive controls overall program function and data flow, while separate functional modules perform defined tasks.

2.4.2 Thermodynamic Engine Model

The Thermodynamic Engine Model has been completed and installed at NASA Lewis. The model has been developed as a simple calculations tool which will take as inputs the three variables: altitude (h), Mach number (M), and power level (PL) on the allowed flight map of an engine, as shown in Figure 5. In addition, ambient temperature deviations from the standard atmosphere, airframe bleed air requirements, and engine deterioration can also be included as part of the input to the thermodynamic model. For each input condition specified by h, M, and PL, the thermodynamic model will calculate gas weight flow ($\dot{w}$), temperature (t), and pressure (p) at selected aerodynamic engine stations as needed to determine component thermal loadings. These stations are shown in Figure 5.

The technique for developing a thermodynamic engine model is shown in Figures 6 and 7. The engine to be analyzed must be defined thermodynamically by an engine cycle deck (computer program) that can be run to generate the internal flow variables at the chosen aerodynamic stations (Figure 6). To encompass the complete engine operating map (Figure 4, 148 operating points are chosen and $\dot{w}$, t, and p are calculated using the cycle deck for the selected stations as well as N_1 and N_2, the fan and core speeds. From this station data, an engine performance cycle map is constructed. This is essentially a set of three-dimensional data arrays that map the station data ($\dot{w}$, t, p, N_1, and N_2) onto the engine operating map (Figure 4). Given an arbitrary operating point defined by h, M, and PL, it is then possible in principle to interpolate on the engine performance cycle map to determine station data. In practice the station parameters are nonlinear functions of

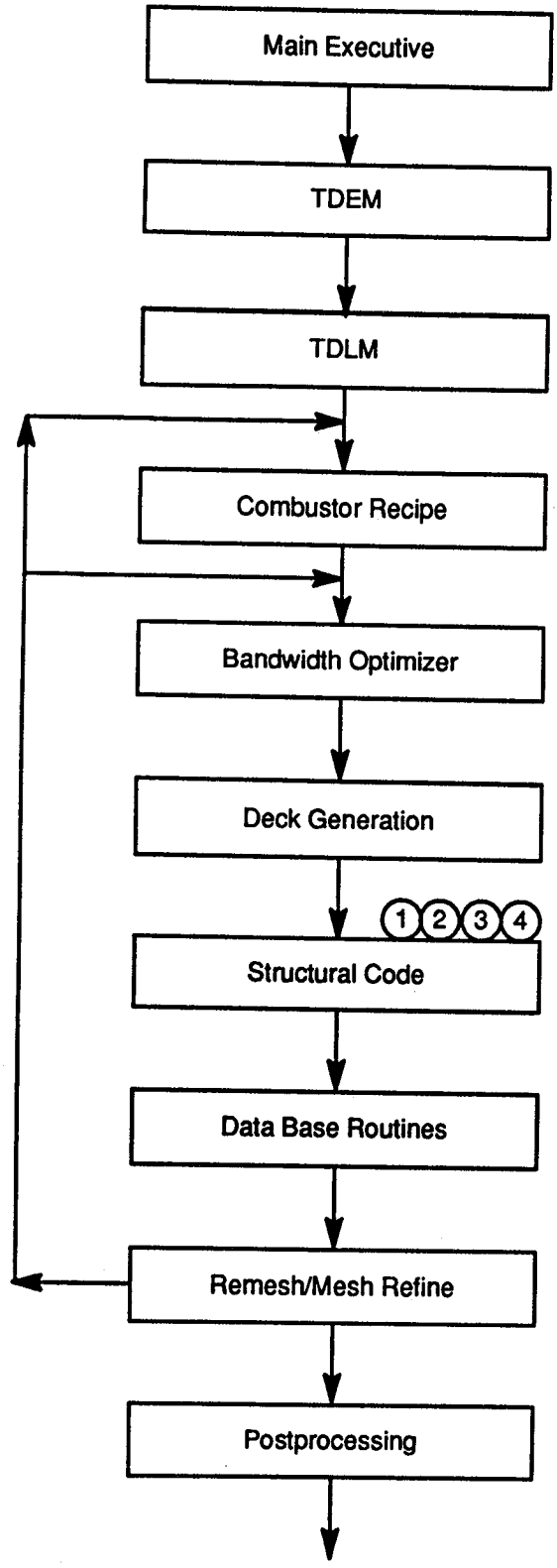

Figure 9. COSMOS System.

the input parameters, and considerable effort is needed to develop these multidimensional interpolations. The computer programs used to generate the engine performance cycle map from the engine cycle desk output has been developed as part of Task III. The functioning of the thermodynamic engine model is shown in Figure 7. Given an engine mission, as shown schematically in Figure 8, it can be defined by values of the input variables h, M, and PL at selected times through the mission. Using these input variables and the engine performance cycle map, an interpolation program developed in this effort will calculate engine station parameters throughout the mission (Figure 7). These are then used to define station mission profiles of $\dot{w}$, t, p, N_1, and N_2 as functions of time at each aerodynamic station. These station mission profiles then become the input to the thermomechanical engine model.

2.4.3 Thermomechanical Loads Model

The Thermomechanical Loads Model is a computer model based on various types of correlations previously developed within GE. For our base program, work has been completed on a generalized procedure that has been established to predict surface temperatures and pressure loads for a rolled ring combustor. This procedure has been developed using all available data arising from both experimental test and analytical methods.

Input for such a model is relatively simple and limited in scope. Geometric information, coupled with heat transfer coefficients and pressure scaling constants, is all combined to define the resulting metal temperatures and pressure loads. A cross-mesh matching algorithm is then employed to map the resulting temperatures and loads to the FEM model generated by the component specific geometric software.

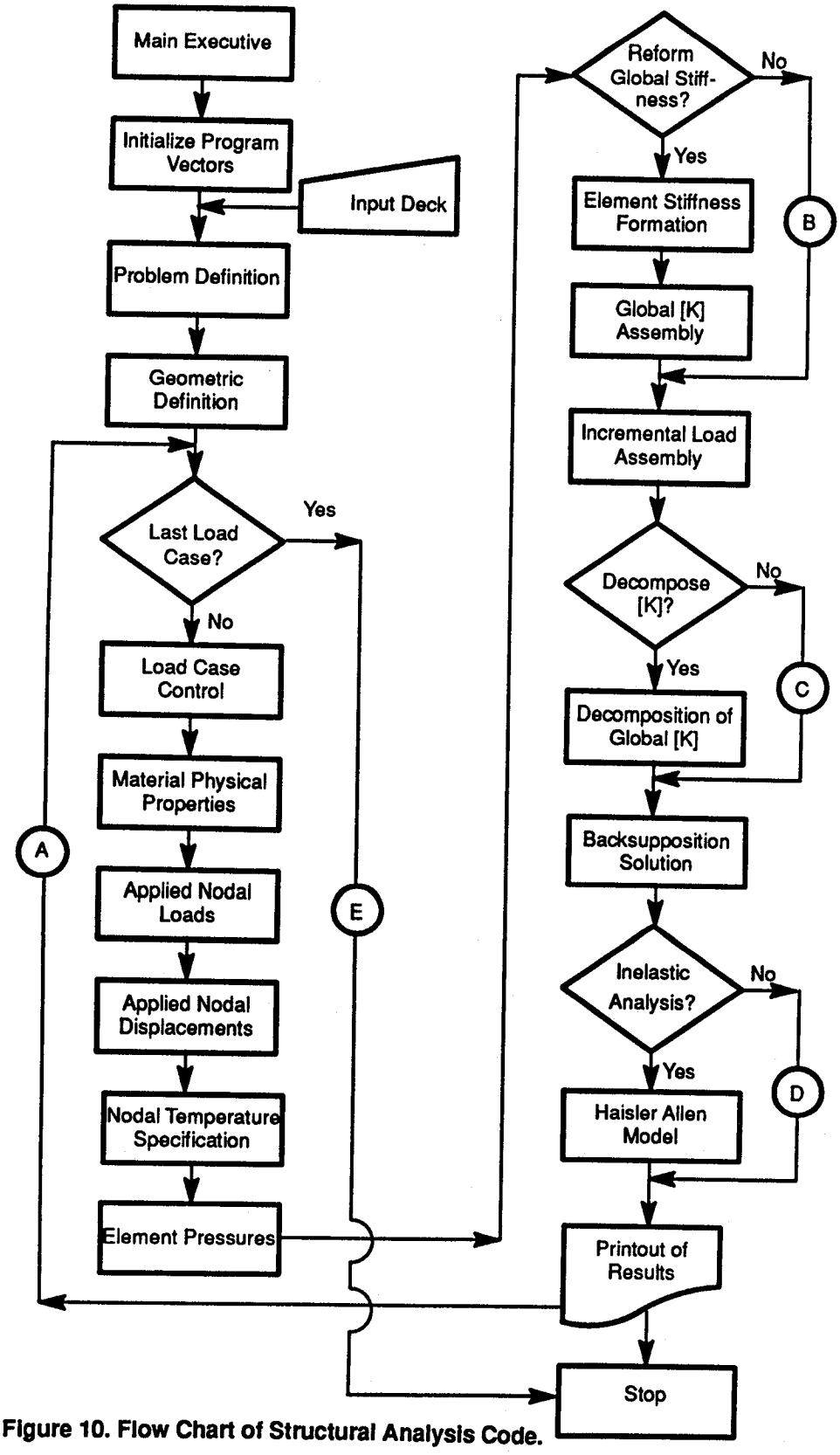

Figure 10. Flow Chart of Structural Analysis Code.

2.4.4 Structural Analysis Code

2.4.4.1 Overview of Attributes & Capability

The structural analysis code developed under this program has been designed to solve complex high temperature thermomechanical problems involving cyclic creep and plasticity. The development of this program has been directed toward its application to the complex geometries, loads, and high temperatures associated with the components within the hot section of gas turbine engines. The finite element code was designed and developed for this contract and is somewhat unique in both its structure and content (Figure 10).

The analysis code is a combination of what we have deemed the most desirable features of many analysis codes into a single entity. Some of these features are presented here.

2.4.4.2 Preprocessing

Preprocessing has been made an integral part of the analysis code. With such capability, the user can instruct the program to read all input and check for errors without having to execute a separate preprocessing type program. The preprocessing function essentially follows the data flow through the analysis code and provides the user a data summary and, in turn, alerts the user to any detected analysis difficulties.

2.4.4.3 Bandwidth Reduction/Optimization

An automated bandwidth reduction algorithm (Gibbs/Poole/Stockmeyer) has been incorporated into the analysis code. This feature may be used as either a selected or a default option. Since most FEM solution algorithms are keyed to bandwidth, a reduction thereon provides the user a more efficient and cost effective solution. The bandwidth reduction algorithm plays an important role in the ability to efficiently and effectively implement remeshing and mesh refinement techniques/algorithms.

2.4.4.4 Internal Numbering System

An internal node and element numbering system is contained within the analysis code. Such a system is extremely useful and affords both the user and the programmer great utility. The user is now free to use numbering systems of convenience and allows for the removal or editing of nodes and elements in the model without affecting the code's overall operation or efficiency.

2.4.4.5 Internal Data Transfer

Much effort was directed towards the efficient storage and retrieval of data within the analysis code. Working information has been grouped into data packets to minimize file manipulation and processing time.

2.4.4.6 Solution Techniques

For reasons of efficiency and problem application dependency, provisions for alternate solution techniques have been included within the analysis code. Currently contained in the analysis code is a COLSOL algorithm with provisions therein for SESOL and FRONTAL techniques.

2.4.4.7 Constitutive Models

The simplified constitutive model and Haisler & Allen's are used to represent inelastic material behavior. Provisions are included in the code to incorporate other constitutive models as they are developed or as they need to be included.

2.4.4.8 Element Library

The twenty noded isoparametric is the element of choice for the demonstration code. The performance of the element for elastic analysis as well as inelastic material applications is well documented. The element stiffness matrix can be computed using either second or third order Gaussian quadrature, but stress recovery is available only at the second order integration points. The eight and sixteen noded isoparametric elements will be incorporated into the code during the follow-on program. Their inclusion will be direct and straightforward owing to the modularity of the overall code.

2.4.4.9 Postprocessing

All postprocessing type functions excluding remeshing and mesh refinement logic are provided via the commercially available, general purpose PATRAN program. All data files required by the PATRAN program are created within the analysis code and are ready for input.

2.5 TASK V - MISSION MODEL DEVELOPMENT

2.5.1 Component Temperature and Pressure Decomposition and Synthesis

Based on the developments described below, a Component Temperature and Pressure Decomposition and Synthesis Plan was approved by the NASA Program Manager. This plan is outlined in Appendix B.

2.5.1.1 Combustor Liner Temperature and Pressure Decomposition and Synthesis

An expression for the temperature gradient through the material thickness can be derived from the cooling effectiveness, the compressor discharge temperature, and the combustor exit temperature. The temperature gradient through the material can be calculated from

$$T_H - T_C = \frac{(Q/A)t}{K} \quad (1)$$

where

T_H = Hot side metal temperature, ^oF

T_C = Cold side metal temperature, ^oF

Q/A = Heat flux through material $\frac{Btu}{hr\text{-}ft^2}$

t = Material thickness, ft.

K = Metal conductivity $\frac{Btu}{ft^2\text{-}hr\text{-}^\circ F/ft}$

The heat flux can be calculated from

$$Q/A = (h_c + h_r)(T_C - T_3) \tag{2}$$

or it is proportional to $(T_{Liner} - T_3)$

$$Q/A = (h_c + h_r)(T_{Liner} - T_3) \tag{3}$$

where

h_c = Convection heat transfer coefficient Btu/hr-ft^2-^{o}F

h_r = Equivalent heat transfer coefficient for radiation to casing

Btu/hr-ft^2-^{o}F

T_{Liner} = Bulk liner temperature, ^{o}F

Substituting the heat flux expression into the gradient equation (1) gives

$$\frac{T_H - T_C}{(T_{Liner} - T_3)} \alpha \frac{(h_c + hr)t}{K} \tag{4}$$

using the equation for cooling effectiveness,

$$y_c = \frac{T_4 - T_{Liner}}{T_4 - T_3} \tag{5}$$

An equation for $(T_{Liner} - T_3)$ can be written as follows:

$$(T_{Liner} - T_3) = (1 - y_c)\ T_4 + (y_c - 1)\ T_3 \tag{6}$$

Substituting Equation 6 into the expression (4) gives

$$\frac{T_H - T_3}{(1 - y_c)\, T_4 + (y_c - 1)\, T_3} \alpha \frac{(h_c + hr)t}{K} \qquad (7)$$

The convection term, h_c, varies with pressure and thus the gradient through the material thickness should be correlated with pressure.

A THTD analysis was done at several pressure conditions and the calculated temperature gradients were plotted vs P3 for several axial locations and the results are shown in Figure 11. The locations and coordinates are shown in Figure 12. As shown in the figure, the gradient data are correlated with pressure. The constants m and b in the equation

$$\frac{T_H - T_C}{T_{Liner} - T_3} = \frac{T_H - T_C}{(1 - y_c)\, T_y + (h_c - 1)\, T_3} = mP_3 + b \qquad (8)$$

are tabulated in Table I.

Table I. Linear Fit Constants for Equation (8).

Location	X, inches	M	b
1	0.094	12.3×10^{-5}	0.100
2	0.438	14.1×10^{-5}	0.061
3	0.654	9.0×10^{-5}	0.061
4	0.854	10.7×10^{-5}	0.092
5	1.114	28.1×10^{-5}	0.168

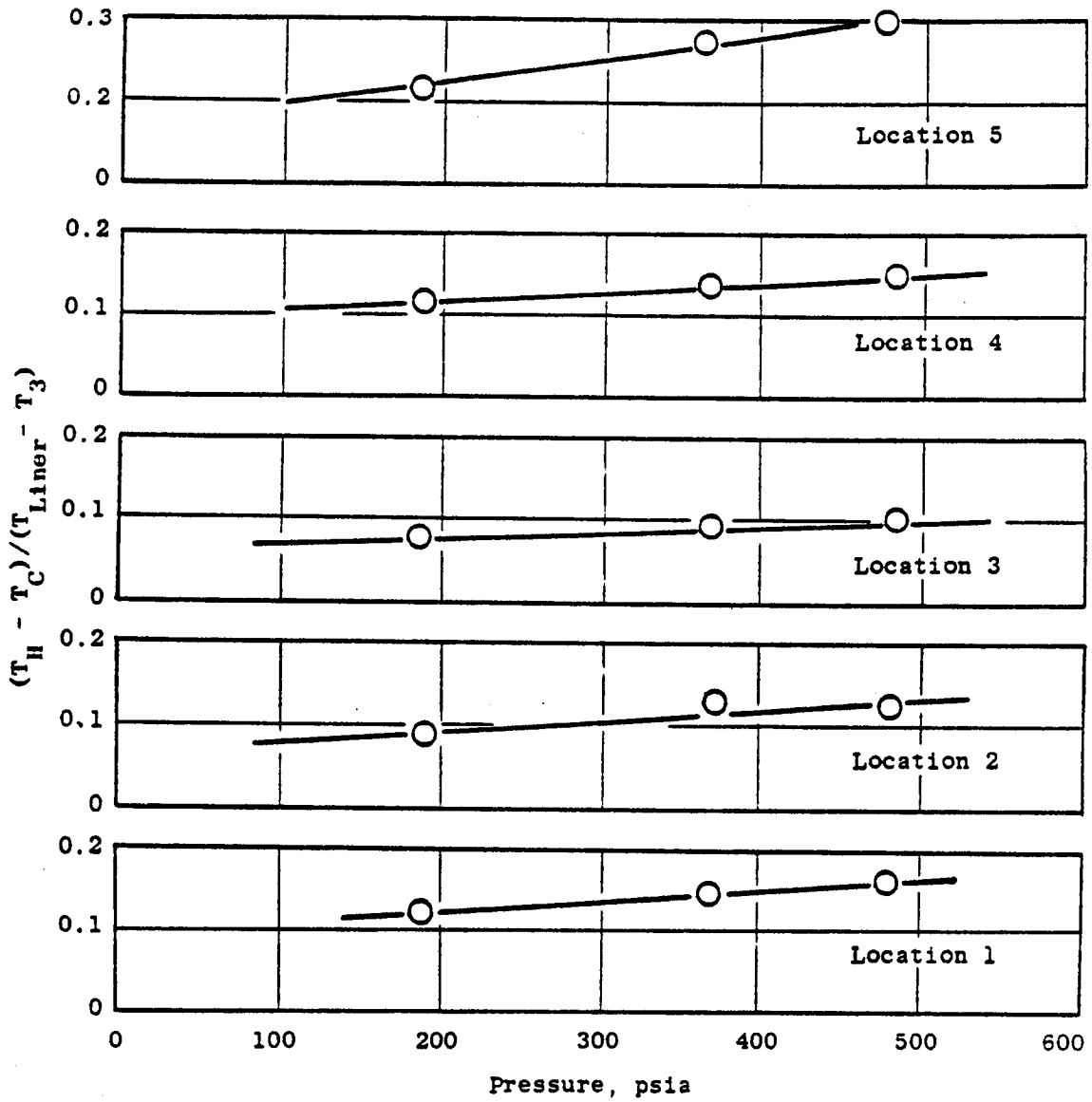

Figure 11. Material Thickness Temperature Gradient.

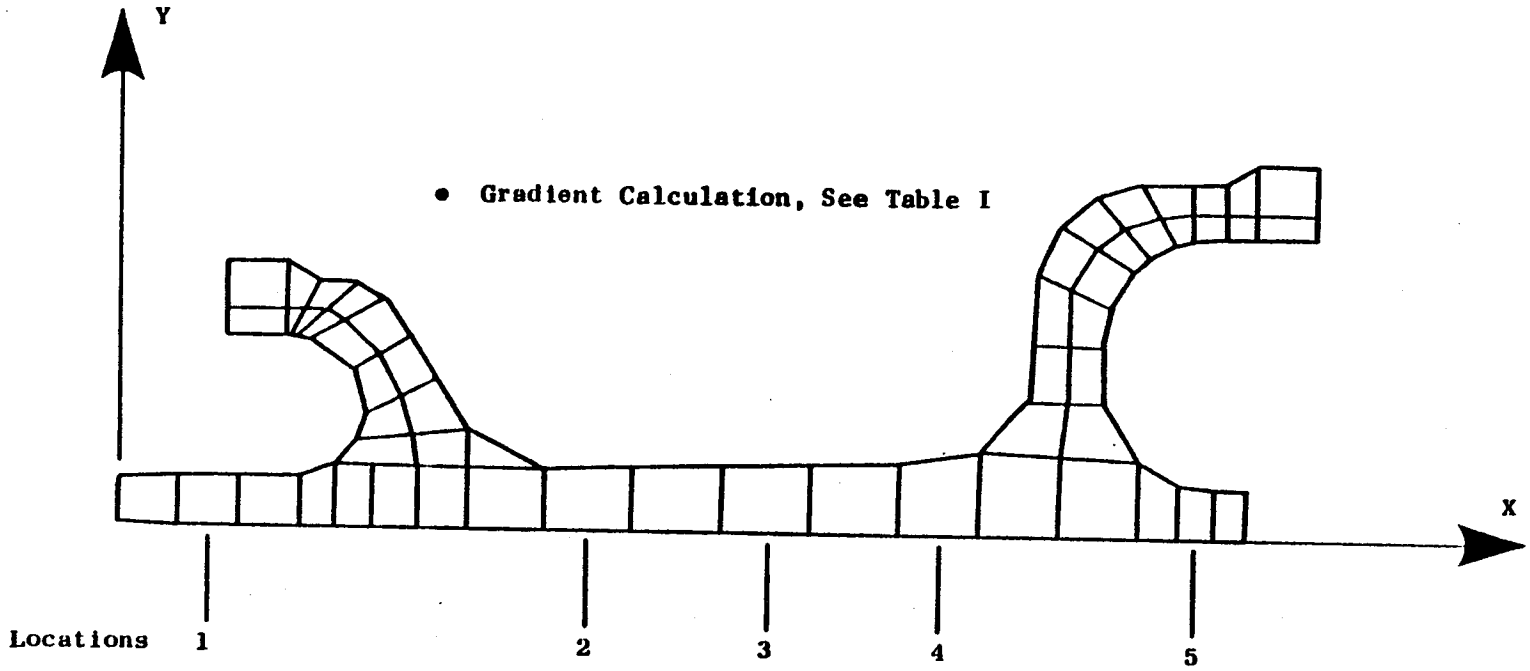

Figure 12. Coordinate System for Cooling Effectiveness.

2.5.1.2 Turbine Blade and Vane Temperature and Pressure Decomposition and Synthesis

The spanwise distribution of overall local cooling effectiveness has been completed for two different Stage 1 HP turbine blades. The results are compared in the attached Figure 13 which is based on Transient Heat Transfer Analysis runs for 15, 50, and 77% of blade span. The ratio of $\eta_{c,local}/\eta_{c,50\%}$ is unity by definition at the 50% span location. At the other two spans, the h_c ratio is identified for each of the sixteen points around the airfoil. The curves have been terminated at the locus or the average h_c ratio for each span.

For the first blade, this procedure defined a single curve for the pressure and suction surfaces. However, the other blade is better represented by a two-branch curve at the 77% span (Figure 14). We have reviewed the two blade designs for possible explanations of this characteristic. There is no obvious single cause. It is undoubtedly the combined result of configuration, coolant circuitry, the application of film cooling and variations in gas-side heat-transfer coefficients.

It appeared best to allow for incorporating separate curves for the pressure and suction surfaces, with freedom to input these curves for different blade designs. This is probably the thing to do for the second blade defining a separate curve for the pressure surface between Points 2 and 6 (Fig. 14). Points 7 and 8 appear to be represented quite well by the curve for the suction surface. Using the suction surface curve for Points 2 through 6 could overpredict the temperatures by about 135^{o}F at the 77% span.

2.6 TASK VI - STRUCTURAL ANALYSIS METHODS EVALUATION

This task was completed during 1983. The selections approved in 2.1 are the result of this effort.

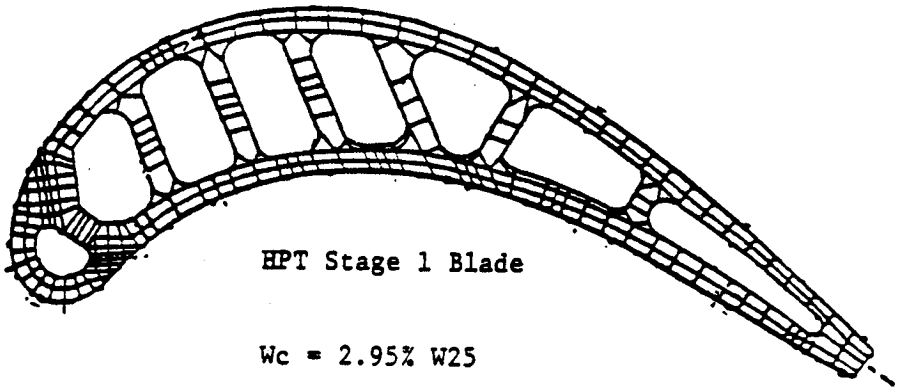

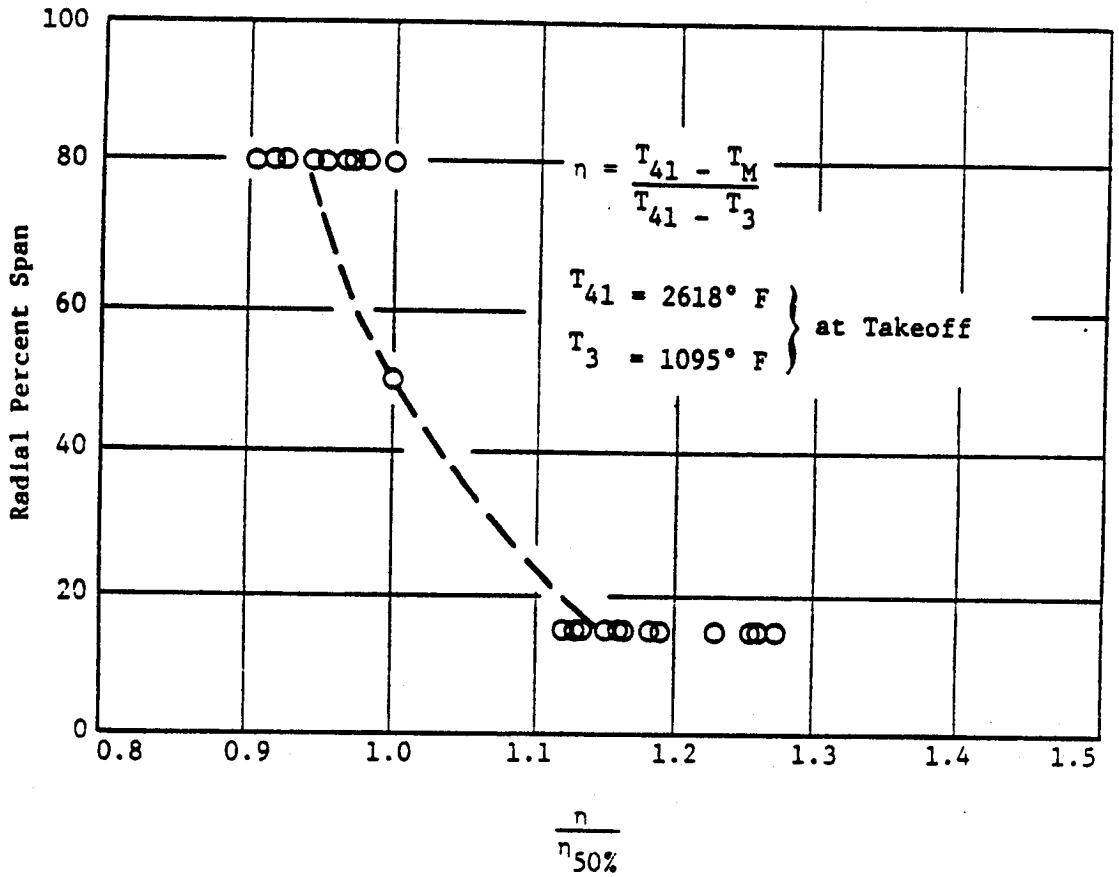

Figure 13. HPT Stage 1 Blade "A" Cooling Effectiveness.

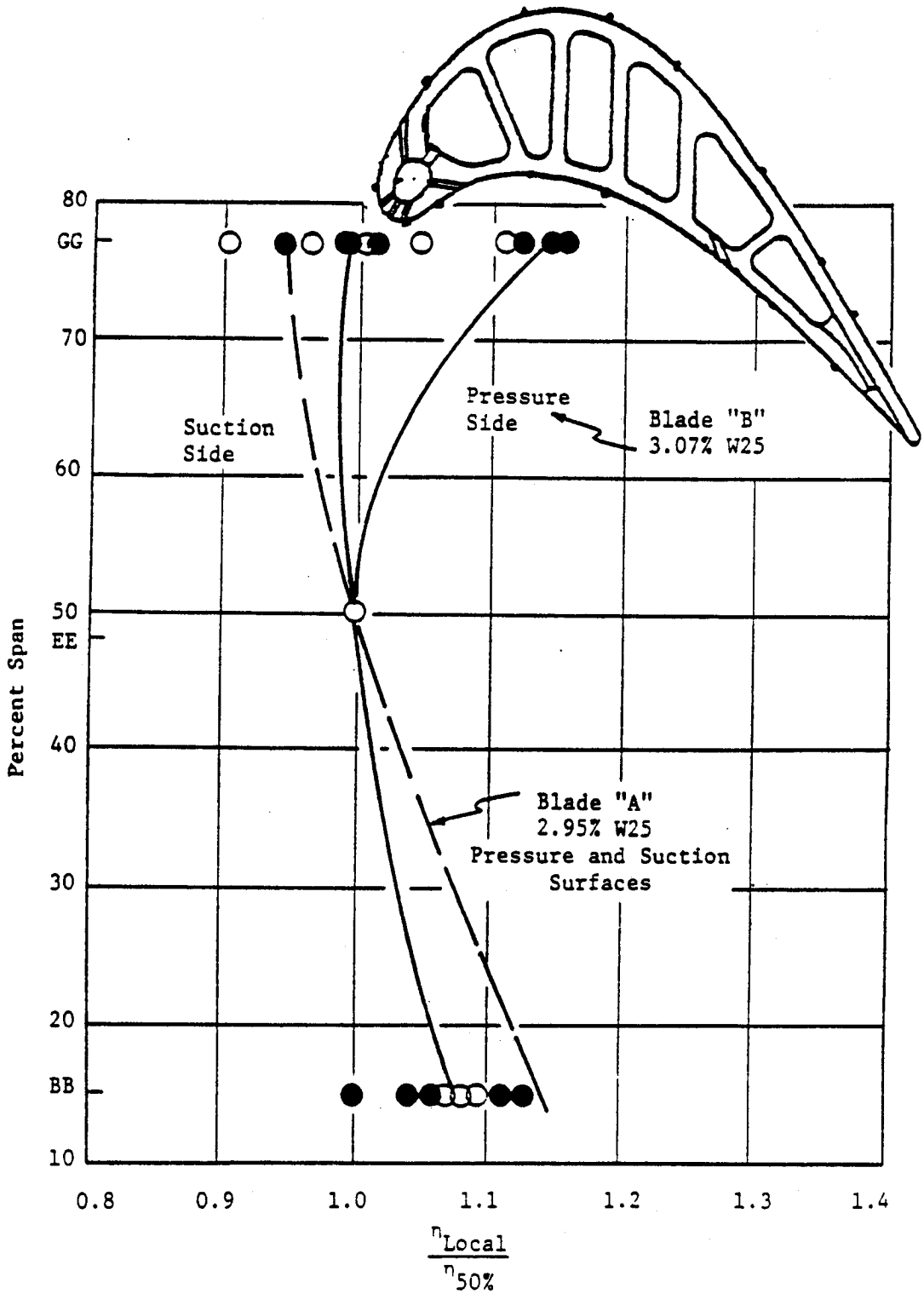

Figure 14. HPT Blade "B" Cooling Effectiveness.

2.7 TASK VII - THERMODYNAMIC LOADS MODEL

Thermodynamic Loads Features for TDE Model:

I. BLADES AND VANES

A. Input is:

1. A series of midspan station temperatures at a specified SS reference case condition, and for each station a percent cord envelope dimension

2. A set of output percent cord envelope dimensions

3. A table of percent radial span versus cooling effectiveness factors. RF, where:

$$RF = \frac{\eta_{cs}}{\eta_{cms}}$$

η_{cs} = cooling effectiveness at specified span dim.

η_{csm} = cooling effectiveness at midspan

The point density in this table will be such that spanwise linear interpolation will suffice.

B. Calculations

1. For each temperature a nominal cooling effectiveness is calculated from:

$$\eta_c = \frac{T41-Tm}{T41-T3}$$

2. At each new condition, all station η_c values are modified by a factor, CF, as follows:

$$CF = \frac{(1 - \eta_c)}{(1 - \eta_c)REF} = ((T3*T41_{REF})/(T3_{REF}*T41))\alpha,$$

where α is input or default value.

3. Output η_c values are linearly interpolated based on percent cord envelope at adjacent input stations.

4. For each output radial distance (specified in the input) all station temperatures are calculated as follows:

$$Tij = T3 + (1 - \eta_{c_R})*CF(T41-T3)*RF$$

Where i = station index

j = radial station index

II. COMBUSTOR

A. Inputs are:

1. Metal bulk node temperatures at axial stations on inner and outer liners, and for each station, x and y dimensions of node centers at a specified reference case condition. Both hot streak and average metal temperature values are input.

2. It is assumed that output node dimensions will match the input nodes.

3. A set of linear equation constants are input for a sparse set of axial locations, identified by "ΔT station" numbers. Output ΔT locations are same as input locations.

4. A set of ΔP scaling constants are input at a sparse set of locations, identified by ΔP station numbers. Output ΔP stations are same as input.

B. Calculations

1. A nominal cooling effectiveness is calculated for each input combustor average and hot streak temperature.

2. At each flight condition, each metal temperature is recalculated from:

$$Tm_{ij} = T3_j + (1 - \eta_{c_i})(T41_j - T3_j)$$

where i = station index and j = flight phase index

3. At each flight condition, each ΔT is recalculated from:

$$\Delta T_{ij} = [T3_j + (1 - \eta_{c_i})(T41 - T3)][b_i + m_i * P3_j]$$

4. At each flight condition, each ΔP is recalculated from:

$$\Delta P_{ij} = P3_j * K_i * \left(\frac{W41}{P3}\right)^2_j * T3_j$$

The accuracy of the thermodynamic engine model has been evaluated, relative to the engine steady-state performance computer model (cycle deck). In a model based on interpolation methods, the maximum error must occur in regions where the "distance" from known data points is greatest. Figure 15 shows the altitude versus Mach number map of stored data points used in the thermodynamic engine model (TEM). The X symbols on this map indicate the worst-case points selected for the error evaluation.

The interpolation logic varies from quadrant to quadrant within a rectangle bounded by stored data points. The nearest point is always used as the base from which the interpolation process is started, for example. Figure 16 shows a typical set of four stored data points. The shaded area is a quadrant. The evaluation test point is at the center. The hypothetical error magnitude curves drawn from two corners to the center illustrate two facts:

- In any quadrant, the error surface is approximately parabolic in shape and maximum at the center of the stored data.

- The four quadrants have different error surfaces, and a discontinuity occurs where they meet.

Since there can be four different maximum error values at each test point, the error analysis was performed four times at each point. The results were summarized by a computer program. The right-hand four columns of Table II show the error values that exceed the target value which is listed in the center of the heading. The left-hand five columns identify the test points. The middle four columns show the accuracy level available before the improvements developed in this program were incorporated. The average of the absolute errors, the max error, and the number of "Exceedances" are given at the bottom of each column. Note that speed, pressure, and horsepower errors are expressed as percent of the rated standard day, sea level value. It seemed more meaningful to express temperature errors in degrees.

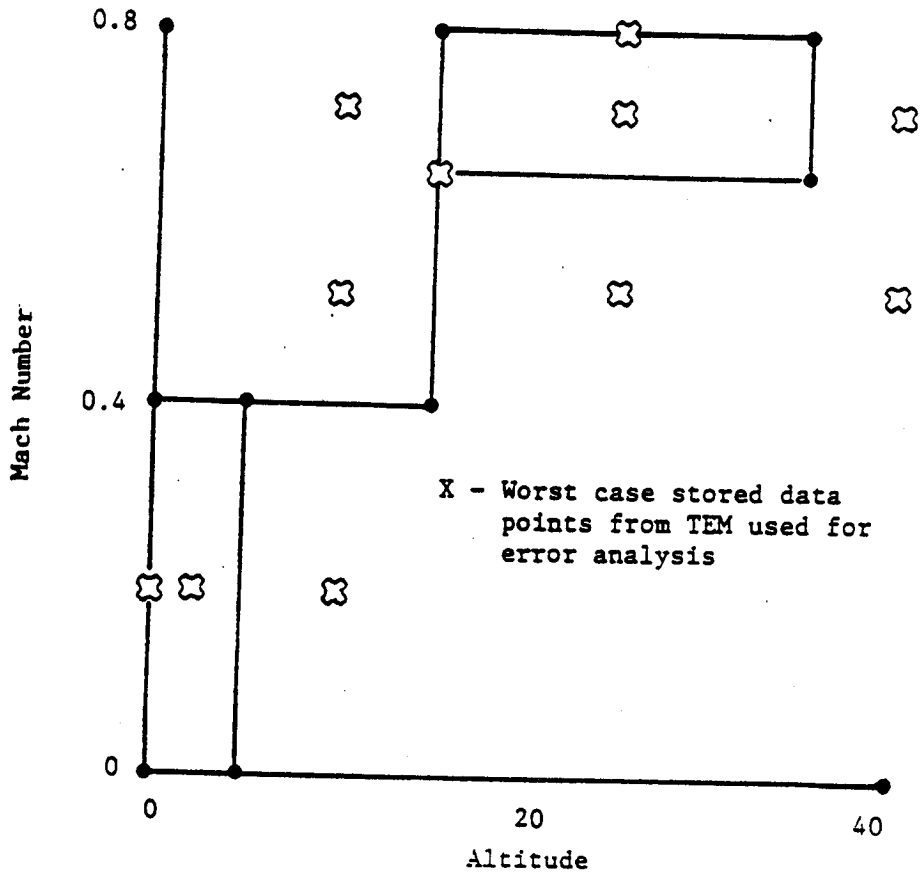

Figure 15. Data Points Used for Interpolation Routines in TEM.

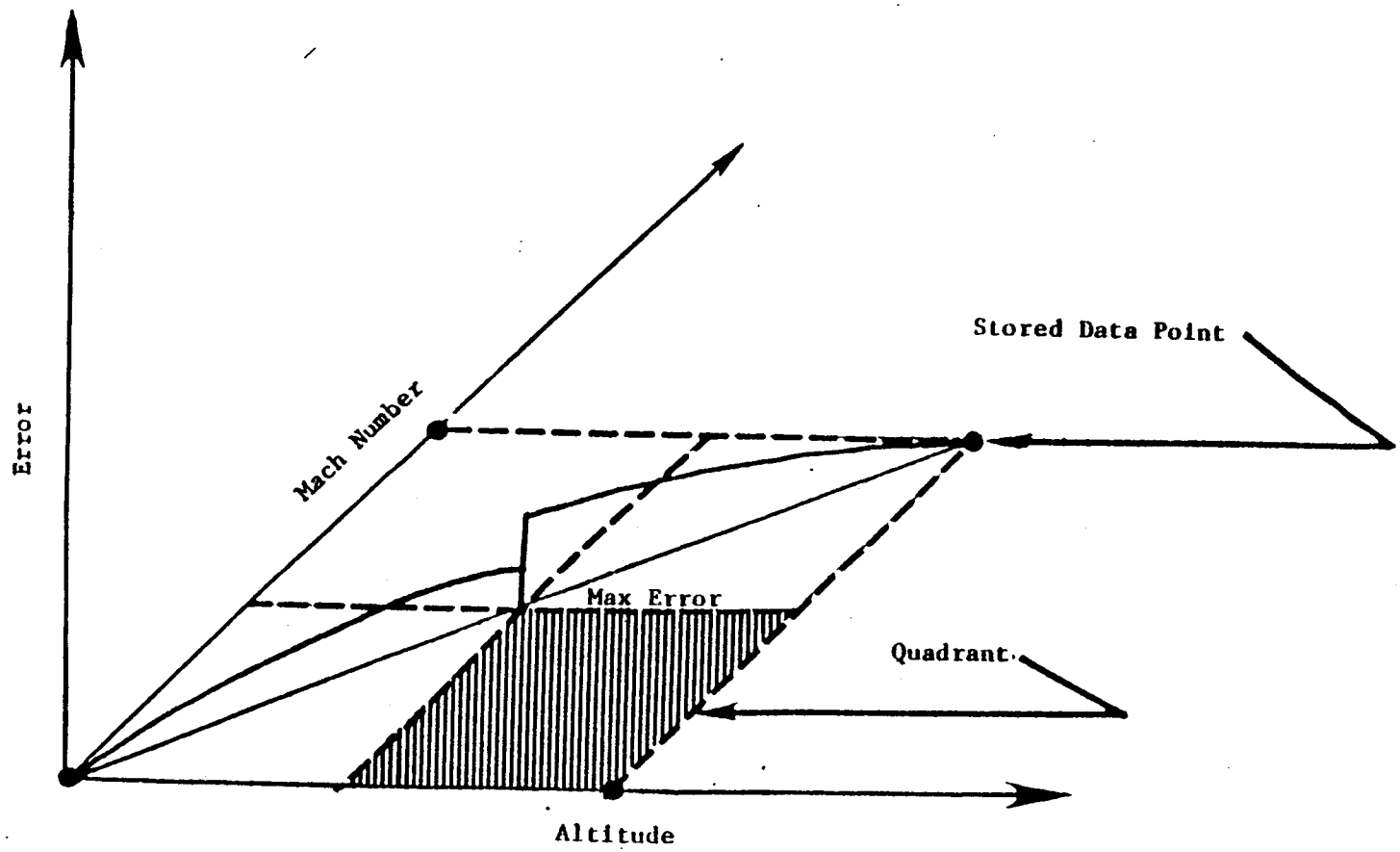

Figure 16. Quadrant Error Distribution.

Table II. Error Summary.

C	MACH	ALT	TB	PCNLR	BLEED	DT48	PERCENT - 0.50							04/04/84
										X N B B				
1	0.20	2500.	513.8680	106	3.2570	-1.0	-0.5510	0.	-0.6205	0.	0.	0.	0.	0.
2	0.20	2500.	513.8620	86	3.1048	-1.0	-0.5046	-0.8857	-0.6877	0.	0.	0.	0.	0.
3	0.20	2500.	513.8620	84	3.1303	-1.0	0.	0.	0.	0.	0.	0.	0.	0.
4	0.20	2500.	513.8620	85	3.0411	-1.0	-1.1888	-1.1591	-0.8959	-0.8267	-0.5578	-0.5565	-0.7176	-0.7855
5	0.20	2500.	513.8620	46	1.9376	-1.0	0.	0.5668	0.	0.	0.	0.	0.	0.
8	0.52	2500.	537.3528	84	3.1620	-1.0	-0.7501	-0.7903	-0.7340	-0.6966	0.	0.	0.	0.
13	0.20	10000.	486.8993	114	2.9939	-1.0	0.	0.	-0.6631	0.	0.	0.	0.	0.
14	0.20	10000.	486.8993	103	2.9303	-1.0	0.	0.	0.	0.	0.	0.	0.	0.
15	0.20	10000.	486.8993	87	2.8686	-1.0	-0.5407	0.	0.	0.	0.	0.	0.	0.
16	0.20	10000.	486.8993	68	1.7500	-1.0	-1.1466	-1.0081	-1.0867	-0.9836	-0.5183	-0.5187	-0.8407	-0.8463
17	0.20	10000.	486.8993	51	1.7500	-1.0	0.	0.	0.	0.	0.	0.	0.	0.
20	0.52	10000.	509.1576	87	2.8930	-1.0	-0.6744	-0.7066	0.	0.	0.	0.	0.	0.
23	0.72	10000.	533.1161	87	2.9232	-1.0	-1.2063	-1.2814	-0.5555	-0.5555	0.	0.	0.	0.
25	0.52	25000.	452.7669	105	2.6150	-1.0	0.	0.	-0.8666	-0.8691	0.	0.	0.	0.
26	0.52	25000.	452.7669	90	1.5000	-1.0	-0.6666	0.	0.	0.	-0.5408	-0.5441	-0.5406	0.
27	0.52	25000.	452.7669	81	1.5000	-1.0	-0.7112	-0.8162	0.	0.	0.	0.	0.	0.
28	0.52	25000.	452.7669	54	1.5000	-1.0	0.	0.6781	0.6806	0.5486	0.	0.	0.	0.
30	0.72	25000.	474.0719	105	2.6430	-1.0	0.	0.	-0.8823	-0.9042	0.	0.	0.	0.
31	0.72	25000.	474.0719	81	1.5000	-1.0	-0.5020	-0.6083	0.	0.	0.	0.	0.	0.
33	0.52	40000.	411.0791	113	2.2351	-1.0	-0.8334	-0.8349	-0.8336	-0.8349	0.	0.	0.	0.
34	0.52	40000.	411.0791	81	1.5000	-1.0	0.	0.	0.	0.	0.	0.	0.	0.
36	0.72	40000.	430.4226	113	2.2623	-1.0	-1.0078	-1.0089	-1.0079	-1.0829	0.	0.	0.	0.
37	0.72	40000.	430.4226	81	1.5000	-1.0	0.	0.	0.	0.	0.	0.	0.	0.
44	0.20	2500.	564.2620	108	3.2390	-1.0	-0.7870	-0.7140	-0.9680	-0.7780	0.	0.	0.	0.
46	0.20	2500.	564.2620	84	3.1178	-1.0	-0.6667	0.	-0.5454	0.	0.	0.	0.	0.
48	0.52	10000.	540.7709	87	2.8857	-1.0	-0.8813	-0.7143	-0.5648	-0.5648	0.	0.	0.	0.
50	0.72	25000.	507.1823	105	2.6368	-1.0	0.	0.	-1.4901	-1.3968	0.	0.	0.	0.
51	0.72	25000.	507.1823	81	1.5000	-1.0	0.	-0.5806	0.	0.	0.	0.	0.	0.
53	0.20	2500.	463.4620	106	3.2789	-1.0	-0.6021	-0.6373	-0.6777	0.	0.	0.	0.	0.
54	0.20	2500.	463.4620	84	3.1446	-1.0	-0.5541	0.	-0.5280	0.	0.	0.	0.	0.
57	0.62	10000.	488.0769	87	2.8983	-1.0	-0.7158	-0.7473	0.	0.	0.	0.	0.	0.
59	0.72	25000.	451.9983	105	2.6489	-1.0	0.	0.	-0.7767	-0.6906	0.	0.	0.	0.
60	0.72	25000.	451.9983	81	1.5000	-1.0	-0.6467	-0.7383	0.	0.	0.	0.	0.	0.
62	0.20	2500.	513.8620	106	3.0626	26.0	-0.6786	-0.8130	-0.8573	-0.6909	0.	0.	0.	0.
63	0.20	2500.	513.8620	84	2.9088	25.0	0.	0.	0.	0.	0.	0.	0.	0.
66	0.62	10000.	509.1575	87	2.7726	26.0	-0.8360	-0.8688	0.	0.	0.	0.	0.	0.
68	0.72	25000.	474.0719	105	2.6327	26.0	0.	0.	-1.3583	-1.2696	0.	0.	0.	0.
69	0.72	25000.	474.0719	81	1.5000	26.0	0.	-0.5976	0.	0.	0.	0.	0.	0.
71	0.20	2500.	513.8620	106	0.3914	-1.0	0.	0.	0.	0.	0.	0.	0.	0.
72	0.20	2500.	513.8620	84	0.2628	-1.0	0.	0.	0.	0.	0.	0.	0.	0.
75	0.52	10000.	508.1575	87	0.2406	-1.0	0.	0.	0.	0.	0.	0.	0.	0.
77	0.72	25000.	474.0719	105	0.8226	-1.0	0.	0.	0.	0.	0.	0.	0.	0.
78	0.72	25000.	474.0719	81	0.1363	-1.0	0.	0.	0.	0.	0.	0.	0.	0.
81	0.20	0.	522.8496	90	0.3171	-1.0	0.	0.	0.	0.	0.	0.	0.	0.
82	0.20	0.	522.8496	56	0.1548	-1.0	0.	0.	0.	0.	0.	0.	0.	0.
84	0.80	25000.	484.5183	104	0.2333	-1.0	0.	0.	0.	0.	0.	0.	0.	0.
85	0.80	25000.	484.5183	65	0.0961	-1.0	0.	0.	0.	0.	0.	0.	0.	0.
87	0.40	5000.	496.2563	84	0.3148	-1.0	0.	0.	0.	0.	0.	0.	0.	0.
88	0.40	5000.	496.2563	57	0.1455	-1.0	0.	0.	0.	0.	0.	0.	0.	0.
89	0.66	15000.	488.8281	108	0.3280	-1.0	0.	0.	0.	0.	0.	0.	0.	0.
90	0.66	15000.	488.8281	84	0.2561	-1.0	0.	0.	0.	0.	0.	0.	0.	0.
91	0.66	15000.	488.8281	59	0.1164	-1.0	0.	0.	0.	0.	0.	0.	0.	0.
92	0.40	5000.	518.8968	114	0.8197	26.0	0.	0.	0.	0.	0.	0.	0.	0.
93	0.40	5000.	518.8968	84	0.1568	26.0	0.	0.	0.	0.	0.	0.	0.	0.
94	0.40	5000.	518.8968	87	0.0718	26.0	0.	0.	0.	0.	0.	0.	0.	0.
					AVG		0.8828	0.8850	0.8876	0.8886	0.1185	0.1064	0.1119	0.1194
					MAX		-1.8863	-1.8814	-1.4901	-1.3968	-0.5578	-0.5565	-0.8407	-0.8463
					NVAL		88	81	81	18	3	3	3	8

Table III shows a brief summary of the accuracy level achieved. Column 2 shows the average of all test point errors. Columns 3, 4, and 5 show the value that is exceeded 2, 4, and 11 times (1%, 2%, and 5% of the 220 error values). Note that all data in this figure refers to the worst-case test points. Since the error surfaces are approximately parabolic in shape, the average error in each quadrant is approximately half of the maximum error, and the overall error is approximately half of the average error listed.

Table III. Validation Case Error Analysis.

		Error Exceeded N Times		
	Average	N = 2	N = 4	N = 11
P_2	0.03%	<1%	<1%	<1%
P_3	0.23%	1.3%	1.2%	1.0%
FNIN1	0.49%	1.8%	1.8%	1.8%
XN25	0.17%	0.7%	0.6%	0.5%
T_2	0.08%	$<5^{o}$	$<5^{o}$	$<5^{o}$
T_3	2.1^{o}	$<10^{o}$	$<10^{o}$	$<10^{o}$
T_{41}	11^{o}	47^{o}	47^{o}	35^{o}

The maximum error of 47^{o}F listed for T41 may seem large. This was one of the most difficult parameters to fit. However, note that 47^{o} is only 2% of the rated T41 value (expressed in ^{o}F) and the true average error is only approximately 0.23%. A User's Manual has been written.

2.8 TASK VIII - COMPONENT SPECIFIC MODEL DEVELOPMENT

2.8.1 Geometric Modeling

2.8.1.1 Combustor Liner Nugget Model

The objective of this subtask was to develop and implement an integrated procedure that would allow the user to create a 3D finite element model of a sector of a combustor liner. The software developed allows the user to interactively create the nugget geometry, maps the thermodynamic engine loads (temperature and pressure) into the geometry, generates both 2D and 3D finite element models and interprets the engine temperatures into the 3D model using the average thermal values and the hot streak values. It also automatically applies the appropriate combustor pressure to the 3D model and generates the symmetric boundary constraints. Finally, it writes this information in a form that is acceptable to the 3D analysis code being used.

The basic nugget geometry is generated using a "geometry recipe" approach. This technique allows the user to generate and control the geometry through a small set of geometrical parameters. These parameters include data which describe the thickness of the liner, the radii of the nugget and the slopes and lengths of key segments in the nugget. Figure 17 shows these parameters and their default values for the liner. Once these parameters are set by the user, the geometry module generates a 2D finite element model representing the liner and the nugget geometry specified. Figure 18 illustrates a typical 2D model with element numbers. The user is then prompted for the thermal/mechanical load input file. This file contains the temperature and pressure data produced by the thermal/mechanical load module for both the average quantities and the hot streak values. Figure 19 shows an example listing of this file. The user is also prompted for the number of fuel nozzles and the number of circumferential elements desired. The module automatically generates a 3D sector model representing an included angle equal to 180^{o} divided by the number of nozzles. The circumferential elemental

Combustor Liner Parameter List

Code	Name	Default	Code	Name	Default
1	X_1	0.0	2	Y_1	0.0
3	α_1	0.0	4	L_1	10.5
5	L_2	2.0	6	L_3	0.5
7	L_4	6.0	8	L_5	0.8
9	L_6	1.0	10	L_7	2.0
11	T_1	0.5	12	T_2	0.7
13	T_3	0.5	14	T_4	0.65
15	T_5	0.5	16	θ_1	90.0
17	θ_2	90.0	18	R_1	1.0
19	R_2	1.0	20	R_3	0.75
21	R_4	1.5	22	R_5	1.5
23	R_6	1.5			

X = Coordinate

Y = Coordinate

α = Angle wrt, x - Axis

L = Length

T = Thickness

θ = Angle of Rotation

R = Radius of Curvature

(n)= Parameter Code Number

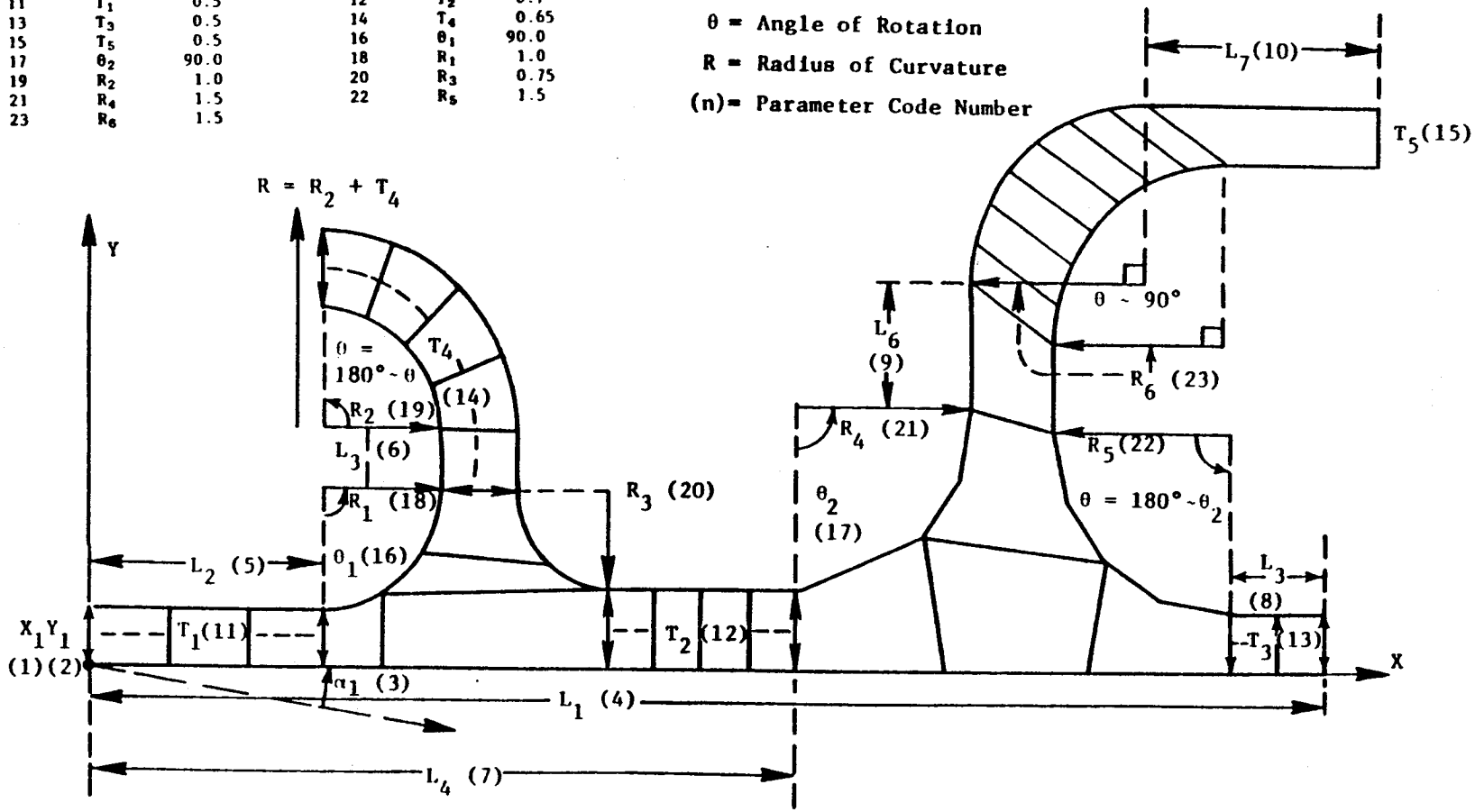

Figure 17. Combustor Liner Parameters.

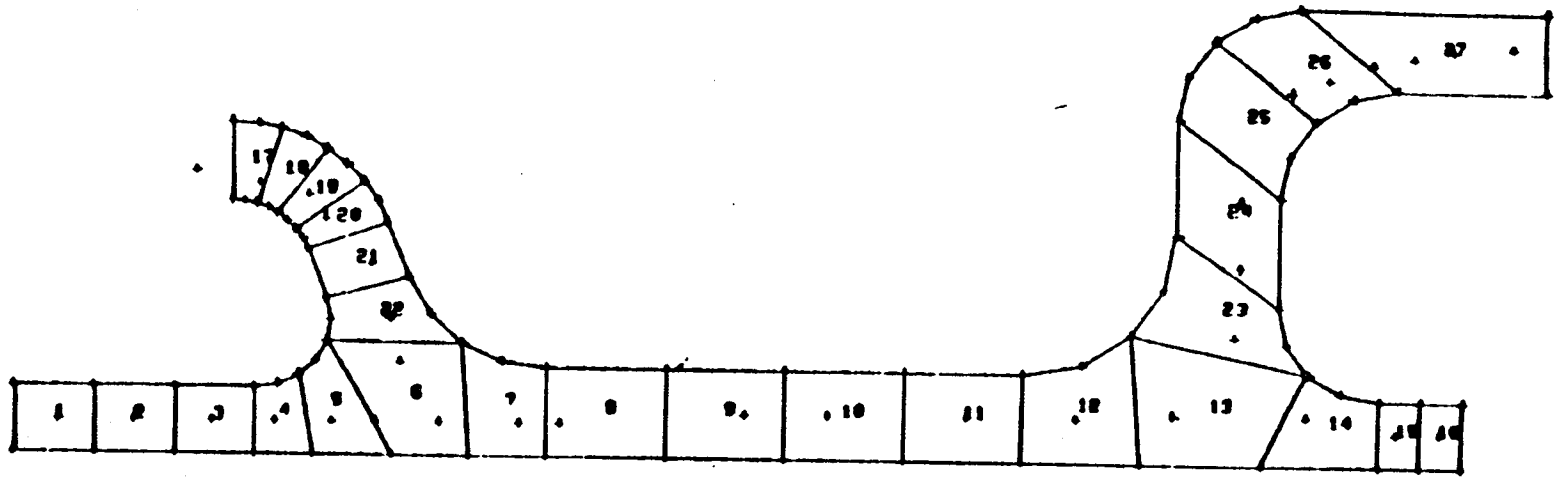

Figure 18. 2D Model Layout

X	Y	T_H	T_A	ΔT_H	ΔT_A	ΔP
0.034	0.030	520.182	520.182	0.161	0.161	0.
0.094	0.030	521.284	521.284	0.263	0.263	0.
0.158	0.030	522.834	522.834	0.391	0.391	0.
0.208	0.030	523.901	523.901	0.463	0.463	0.
0.254	0.030	524.487	524.487	0.485	0.485	0.
0.288	0.030	524.935	524.935	0.499	0.499	0.
0.340	0.030	525.658	525.520	0.516	0.505	0.
0.404	0.030	526.519	526.002	0.523	0.489	0.
0.438	0.030	528.827	526.967	0.639	0.521	0.
0.584	0.040	530.446	527.690	0.735	0.562	0.
0.654	0.040	531.376	528.276	0.790	0.597	0.
0.764	0.040	531.686	528.758	1.032	0.800	0.
0.854	0.040	530.928	527.690	1.144	0.841	0.
0.934	0.044	529.826	527.311	1.310	1.014	0.
1.040	0.044	528.586	526.967	1.481	1.238	0.
1.074	0.040	527.828	526.726	1.461	1.284	0.
1.114	0.030	527.656	526.485	1.541	1.340	0.
1.150	0.030	527.518	526.381	1.613	1.405	0.

Figure 19. Outputs from Combustor Thermodynamic Loads Model.

spacing can be controlled by the user to bias the element toward the hot streak area. The thermal data is mapped sinusoidally from the average to the hot streak plane. The combustor pressures are applied to the appropriate free surfaces and symmetric constraints are generated for the front and back node planes. Figure 20 shows a complete 3D model of the liner. Figure 21 shows the same model with hidden lines removed. Figure 22 shows the typical execution of this module.

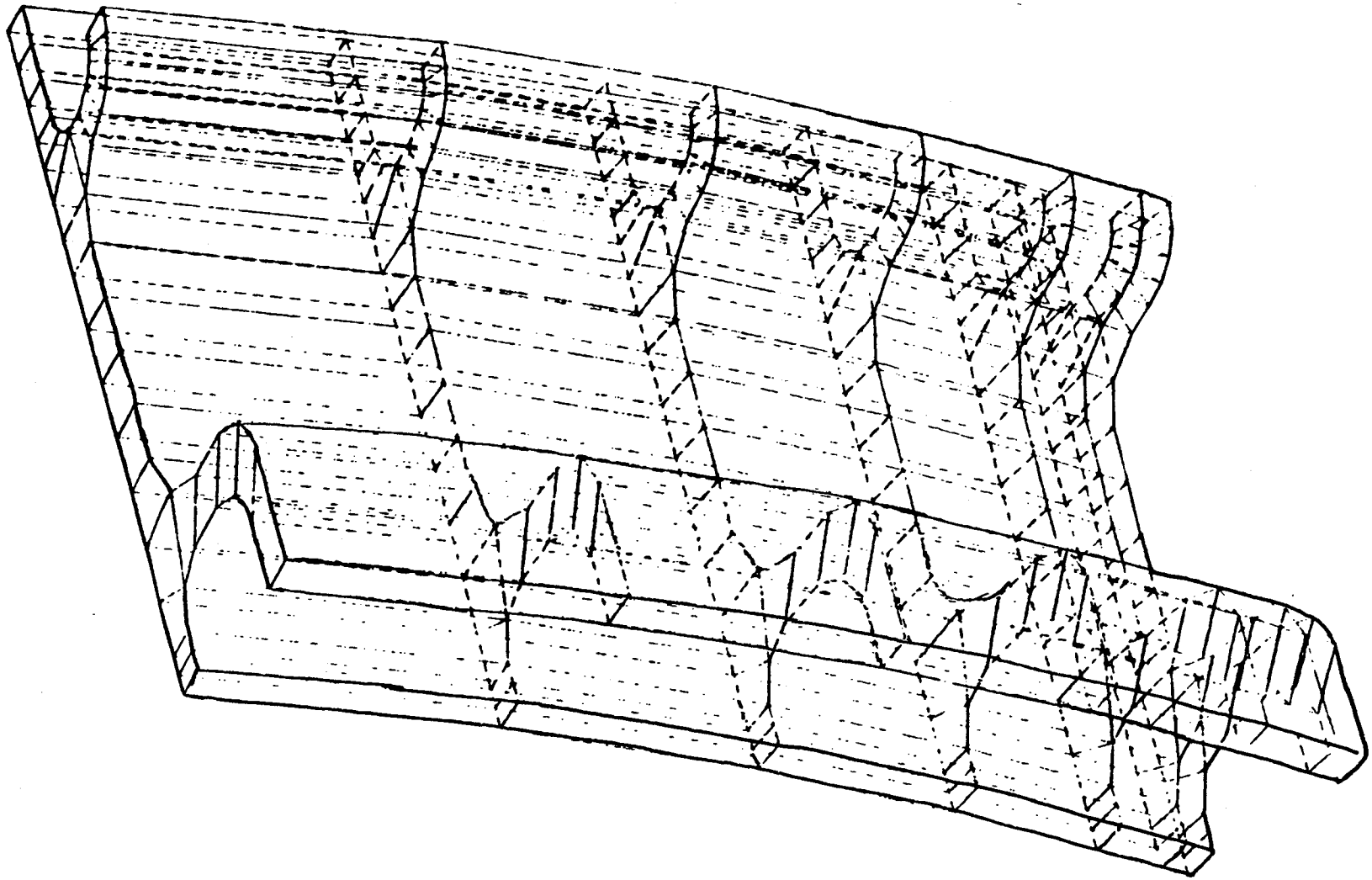

Figure 20. 3D Model Layout.

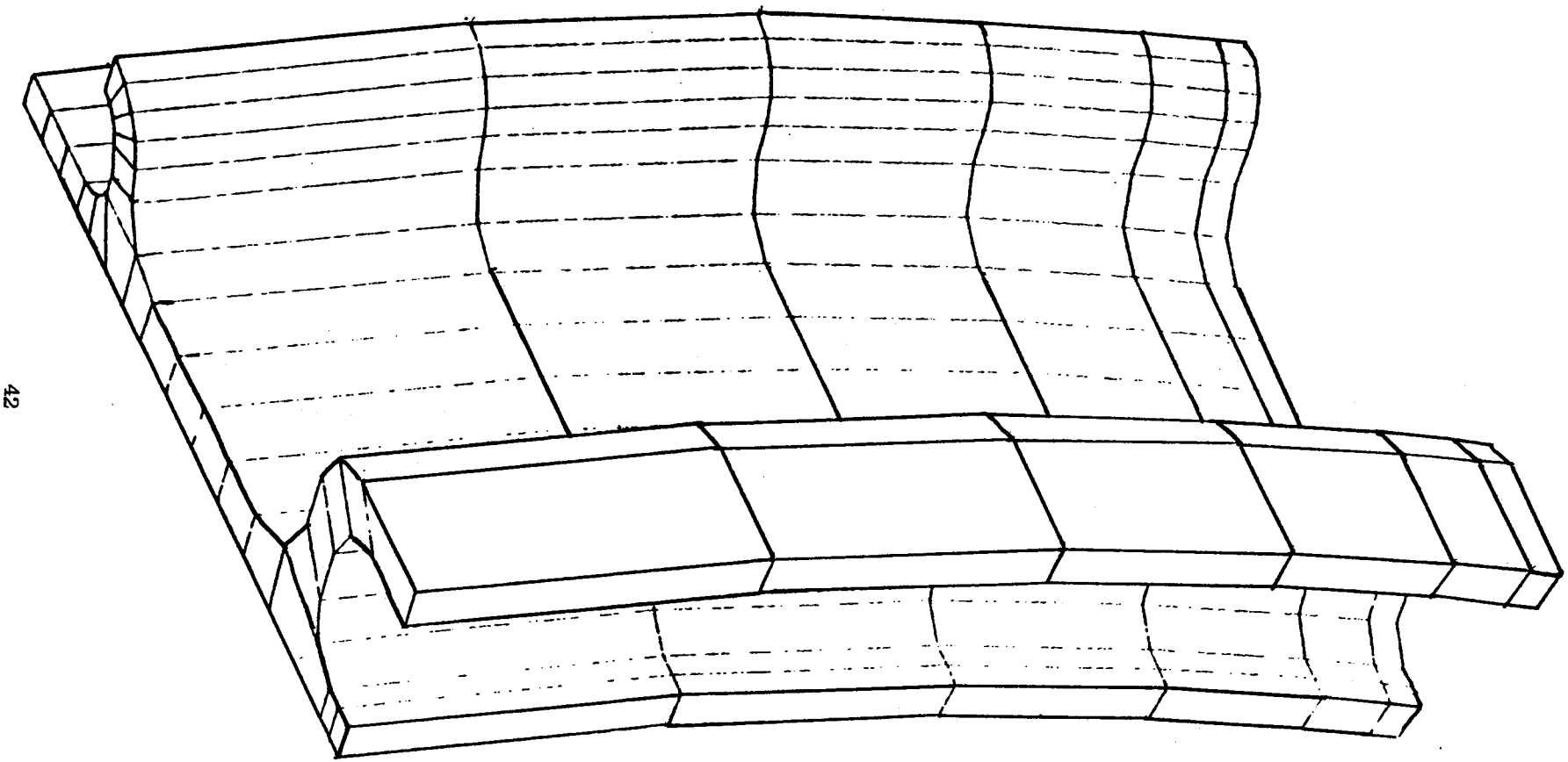

Figure 21. Hidden Line Plot of 3D Model.

```
$/RN /GN/NUGPRO

      NUGGET RECIPE    VERS.II 8/20/85

DO YOU HAVE A PARAMETER FILE ?1? <0/1>
*

          CODE      VALUE                CODE      VALUE
            1         0.                   2         0.
            3         0.                   4     1.16700
            5     0.19200                  6     0.04500
            7     0.81000                  8     0.06800
            9     0.10000                 10     0.20000
           11     0.06000                 12     0.08000
           13     0.06000                 14     0.06800
           15     0.06800                 16   110.00000
           17    90.00000                 18     0.06000
           19     0.06300                 20     0.12000
           21     0.12500                 22     0.08300
           23     0.09500

 ENTER PARAMETER CHANGES (ENTRY CODE, NEW VALUE)
     WHEN DONE ENTER     0 0
*0 0

          CODE      VALUE                CODE      VALUE
            1         0.                   2         0.
            3         0.                   4     1.16700
            5     0.19200                  6     0.04500
            7     0.81000                  8     0.06800
            9     0.10000                 10     0.20000
           11     0.06000                 12     0.08000
           13     0.06000                 14     0.06800
           15     0.06800                 16   110.00000
           17    90.00000                 18     0.06000
           19     0.06300                 20     0.12000
           21     0.12500                 22     0.08300
           23     0.09500

 DO YOU WANT TO CHANGE PARAMETERS? <0/1>
*
READING FILE NUGCON
READING DONE
              27 ELEMENTS READ

ENTER ENGINE TEMPERATURE AND PRESSURE FILE NAME
*/GN/NUGINF
READING FILE /GN/NUGINF
READING DONE
              36 CENTROIDS READ

ENTER THE NUMBER OF EXHAUST NOZZLES
  AND THE NO. OF CIRCUMFIRENTIAL ELEMENTS
  BETWEEN T-AVE AND T-HOT (MAX NO.=10)
*3 4

ENTER THE  3 CIRCUMFIRENTIAL BIASING PARAMETERS
 -- ENTER AS PERCENTS, THE SUM BEING LESS THAN 100% --
*6 15 30

 ********   3192 NODES IN 3-D MODEL      ********
 ********    648 ELEMENTS IN 3-D MODEL   ********
 ********    768 FACES WITH PRESSURES    ********

 ### 2-D NODE  FILE IS TEMP FILE 20 ###
 ### PARAMETER FILE IS TEMP FILE 21 ###
 ### 3-D  UIF  FILE IS TEMP FILE 36 ###
$
```

Figure 22. Typical Program Run.

2.8.1.2 Geometrical Modeling of Turbine Blade and Vanes

The recipe approach was used very successfully for the combustor liner; however, it cannot be used for the blade and vanes due to the significant complexity of the airfoil geometry. A typical multiple cavity turbine blade is shown in Figure 23. There is no reasonable number of physical parameters which could be used to easily describe this geometry. The outside contour of the airfoil is a complex curve defined by aerodynamic requirements. In many cases, the aero analysis is performed prior to or in parallel with the mechanical design, and one of the outputs of the aero analysis is a file of points defining the outer contour of the blade at a number of span locations.

The models developed in this subtask use as input a coordinate file which defines the outer airfoil contour for a maximum of 30 spanwise sections. The number of points per section can vary with a maximum of 60. These limits are parameterized in the code and can be easily adjusted. Figure 24 illustrates a series of points for two spanwise sections.

The code allows the user to specify the number of elements in the spanwise and chordwise directions and also allows for multiple elements through the thickness of the airfoil. The program will automatically evenly space the elements in all three directions or the user can control the biasing of the elements. The basic section input can be modified using built in scaling and offset logic, and the leading and trailing edge thicknesses can be altered through user prompts. The number, size and location of the internal cavities can also be controlled by the user. Figure 25 shows an example of a simple execution of the code.

Figure 26 shows a 3D model comprised of 20-noded isoparametric elements of a solid airfoil created by this module. Figures 27 and 28 represent the same airfoil with two cavities near the leading edge. The plot in Figure 28 is a "free edge" plot that clearly shows the cavity as it passes through the airfoil. Figures 29 and 30 show a model created with three large cavities and three elements across each of the spans. Note that wall thickness of the

airfoil was varied along the span for this example. The final example shown in Figures 31 and 32 illustrates how the spanwise and chordwise element biasing can be used in conjunction with a variable layer thickness. Once again, the output of this module is a file containing 20-noded solid elements compatible with the 3D nonlinear code developed as a part of this contract.

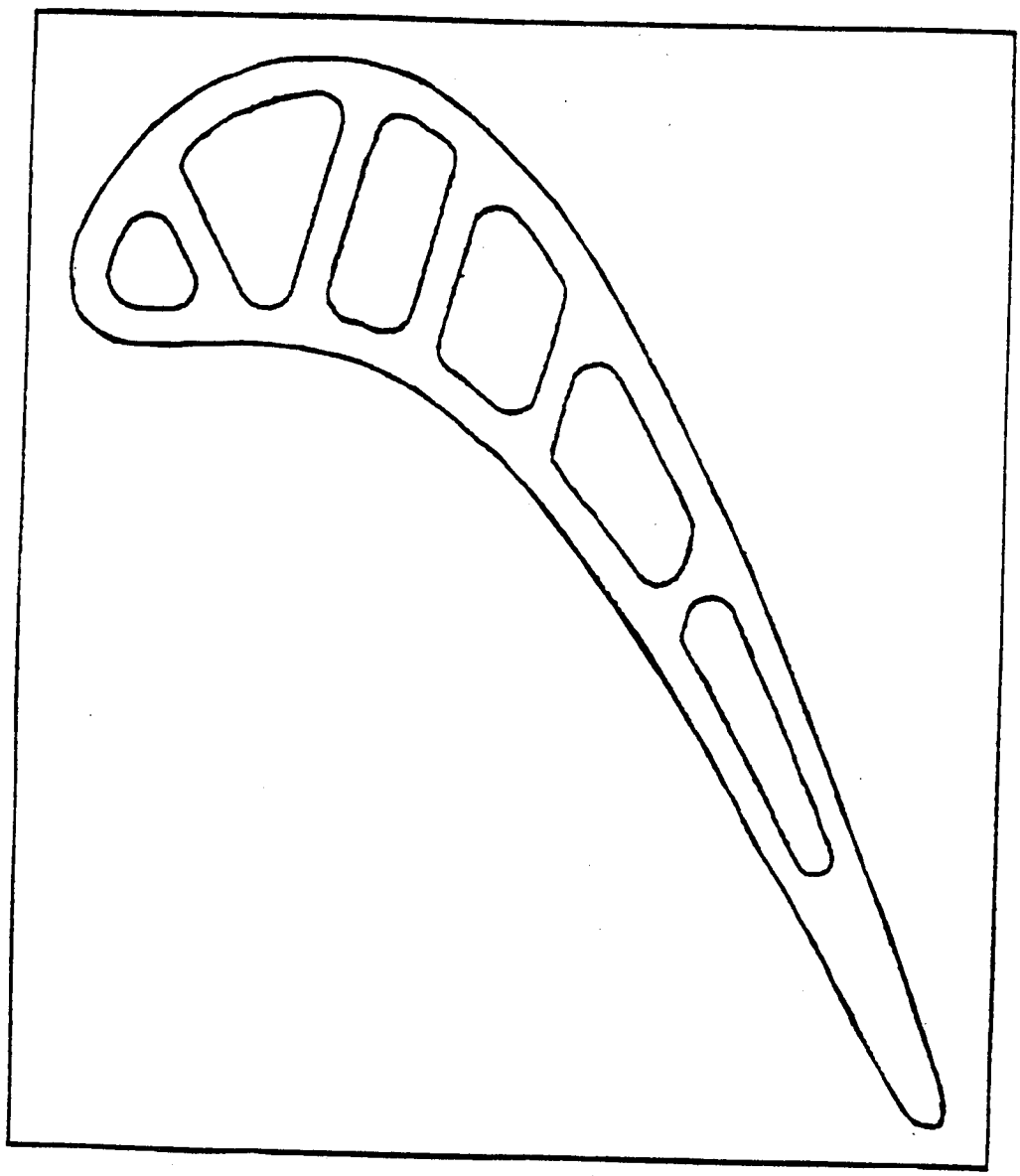

Figure 23. Cooled Turbine Blade Cross Section.

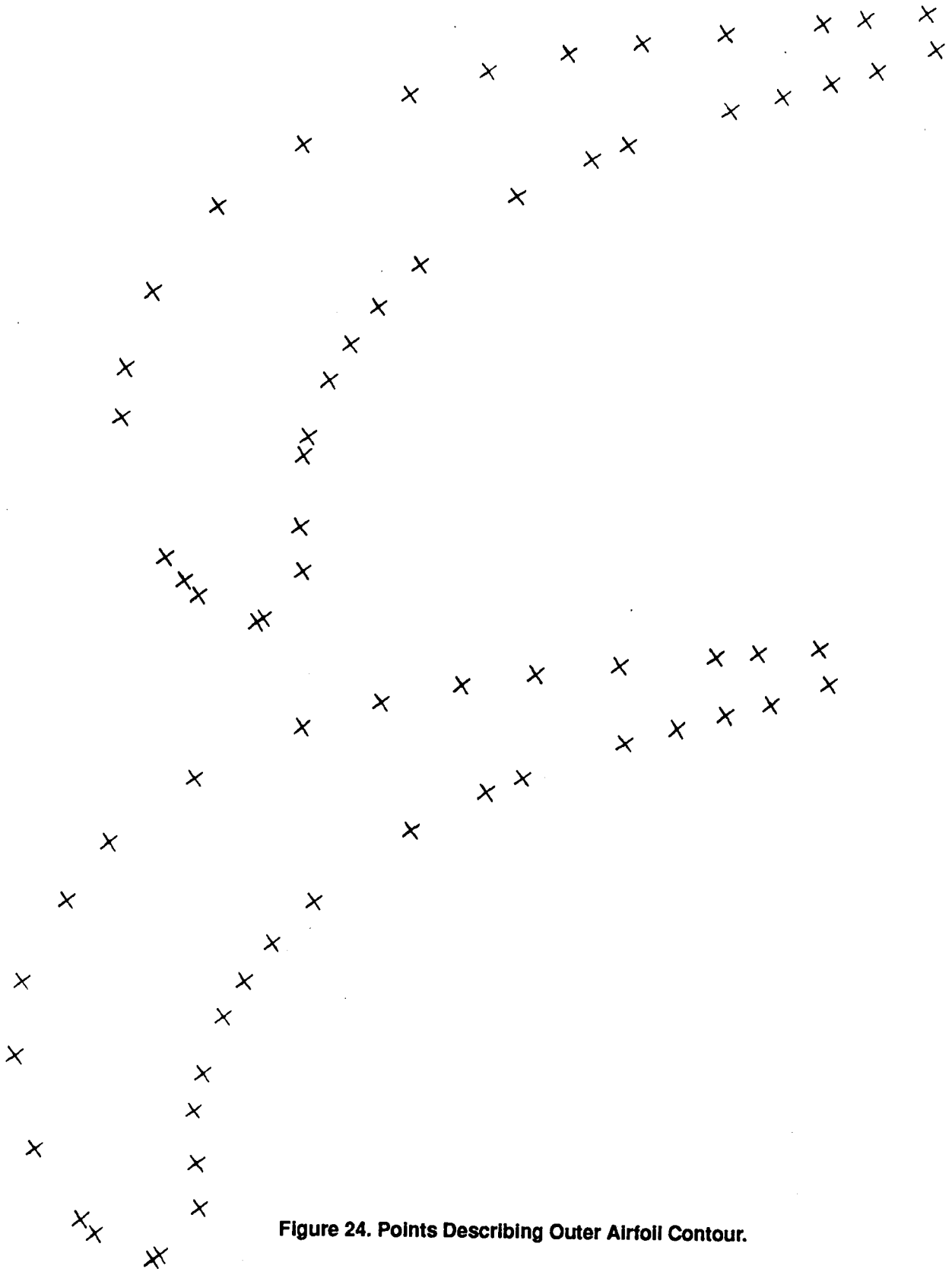

Figure 24. Points Describing Outer Airfoil Contour.

```
TITLE=                                        DATE =10/21/86      TIME = 12.02      PAGE= 1

##################################################
         COMPONENT SPECIFIC AIROIL GENERATOR
##################################################
INPUT AIRFOIL FILENAME
=AERO2
HOW MANY PAIRS OF POINTS IN EACH CROSS SECTION?
=17
HOW MANY DIGITIZED SECTIONS
=2
TYPE 1 TO MODIFY THE INPUT DATA
=0
HOW MANY ELEMENTS ALONG CHORD ?
=10
TYPE 1 FOR USER DEFINED SPACING
=0
SECTION  1 UNWRAPPED CHORD  1.8337
SECTION  2 UNWRAPPED CHORD  1.8316
HOW MANY ELEMENTS ALONG SPAN ?
=5
HOW MANY ELEMENTS ACROSS THE THICKNESS
=3
TYPE O FOR THE EQUALLY SPACED METHOD
TYPE 1 FOR THE MULITPLE COATING (SKIN) METHOD
=0
ENTER THE NUMBER OF CAVITY LAYERS
=1
ENTER THE NUMBER OF CAVITY ELEMENT ROWS
  AND THE ELEMENT CAVITY ROW NUMBERS
=2 3 5

 YOUR UIF IS ON FILE 31
  NO. OF NODES   ,LAST NODE        =  922  922
  NO. OF ELEMENTS                  =  140
```

Figure 25. Simple Example of Airfoil Generator Execution.

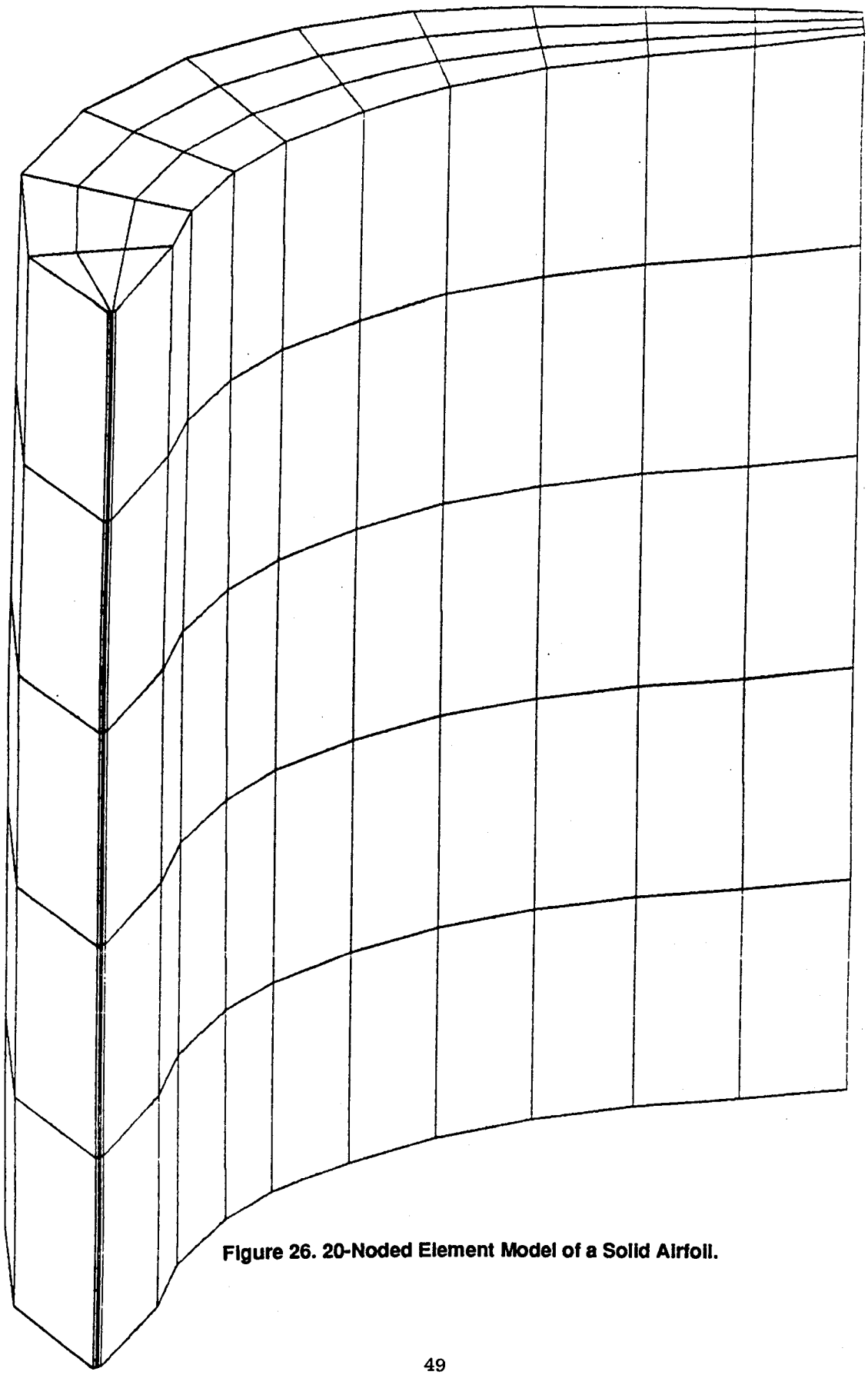

Figure 26. 20-Noded Element Model of a Solid Airfoil.

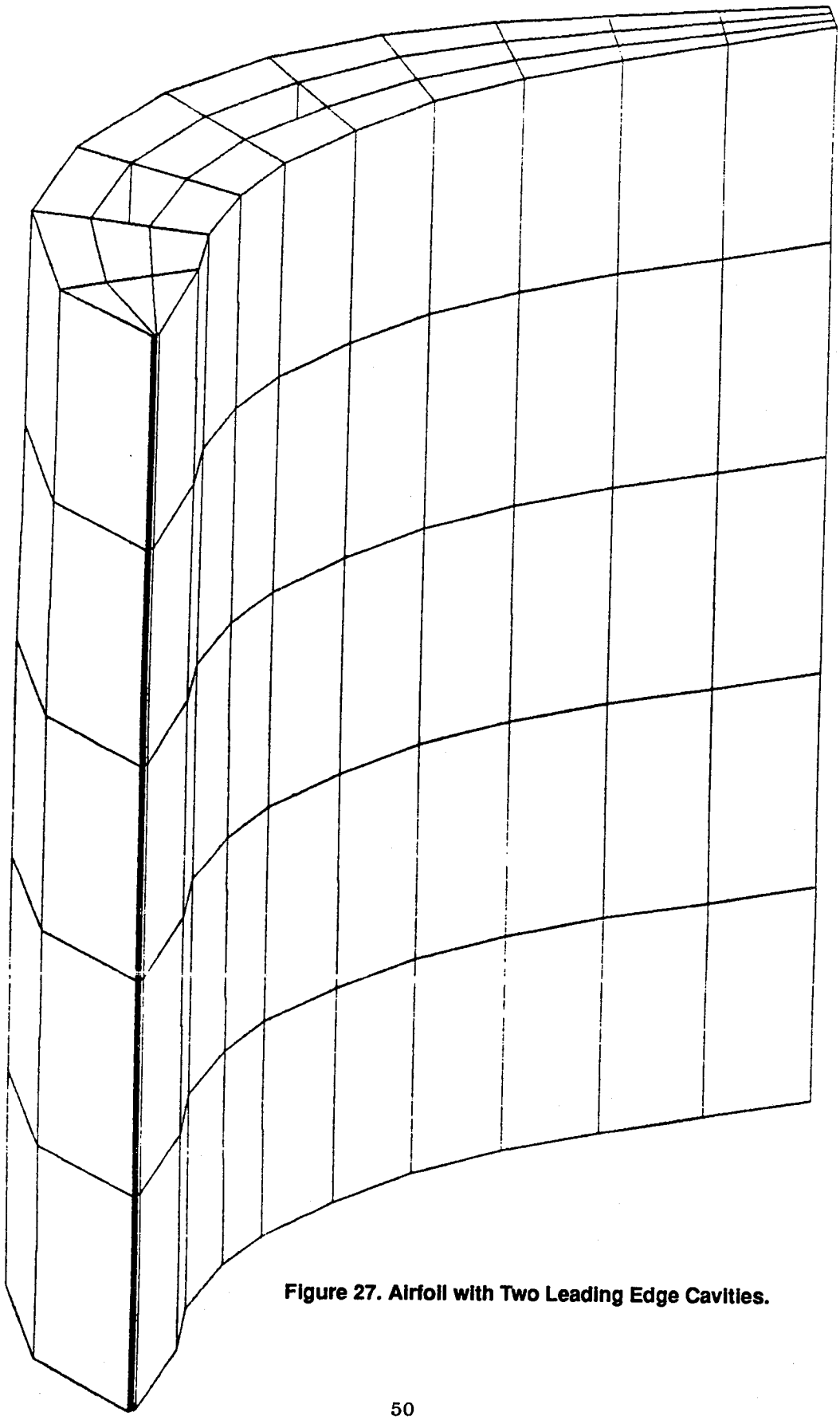

Figure 27. Airfoil with Two Leading Edge Cavities.

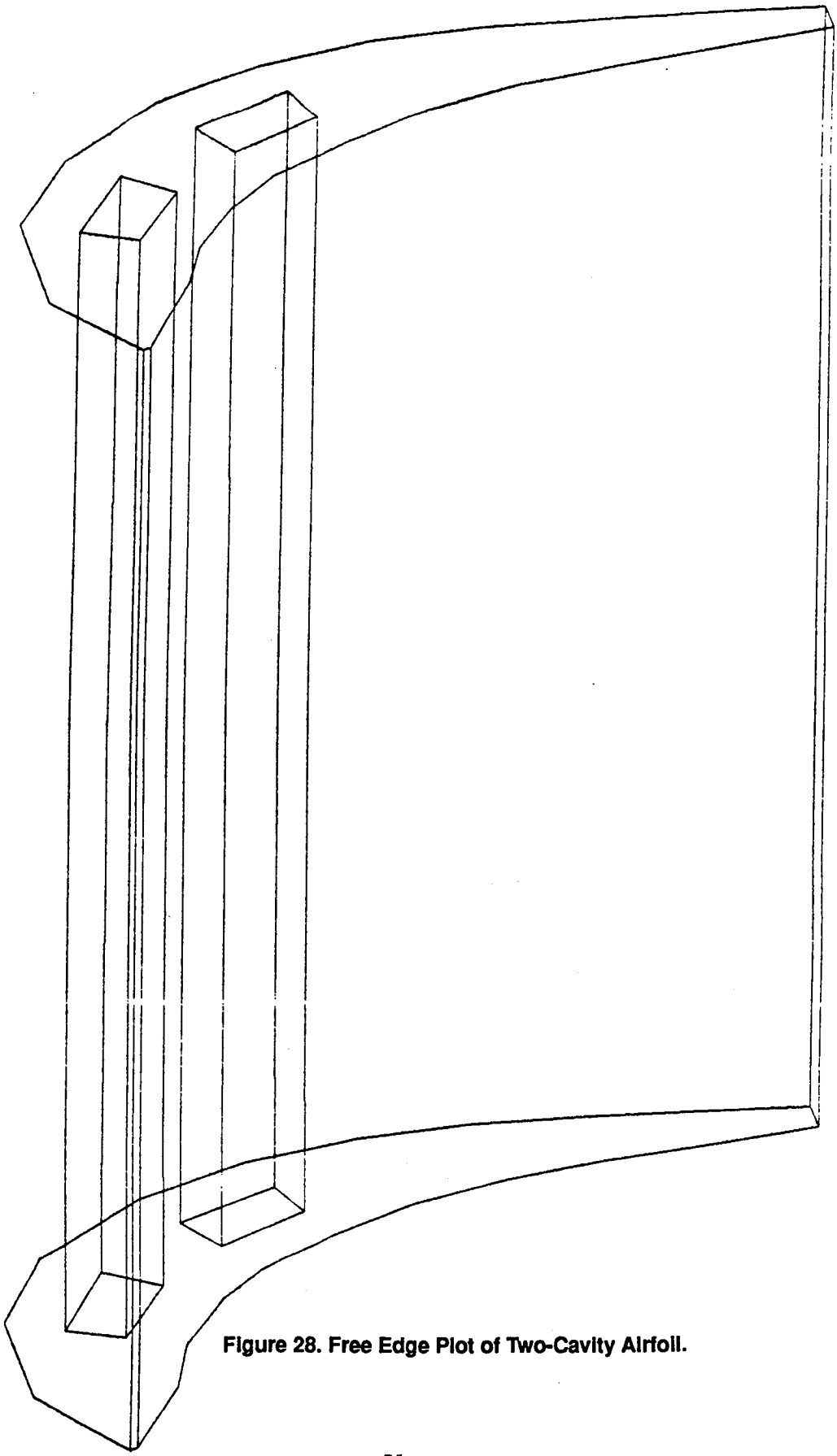

Figure 28. Free Edge Plot of Two-Cavity Airfoil.

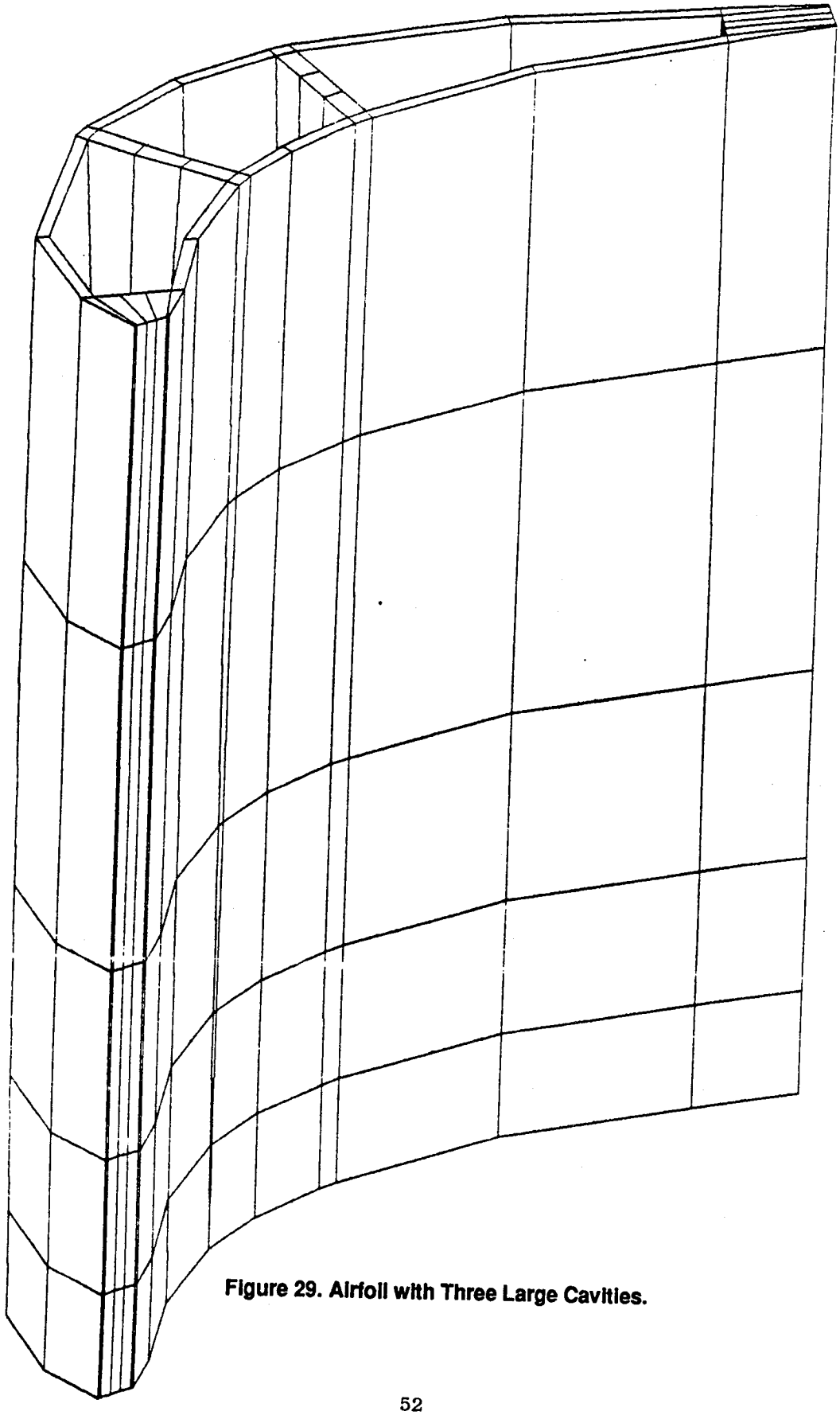

Figure 29. Airfoil with Three Large Cavities.

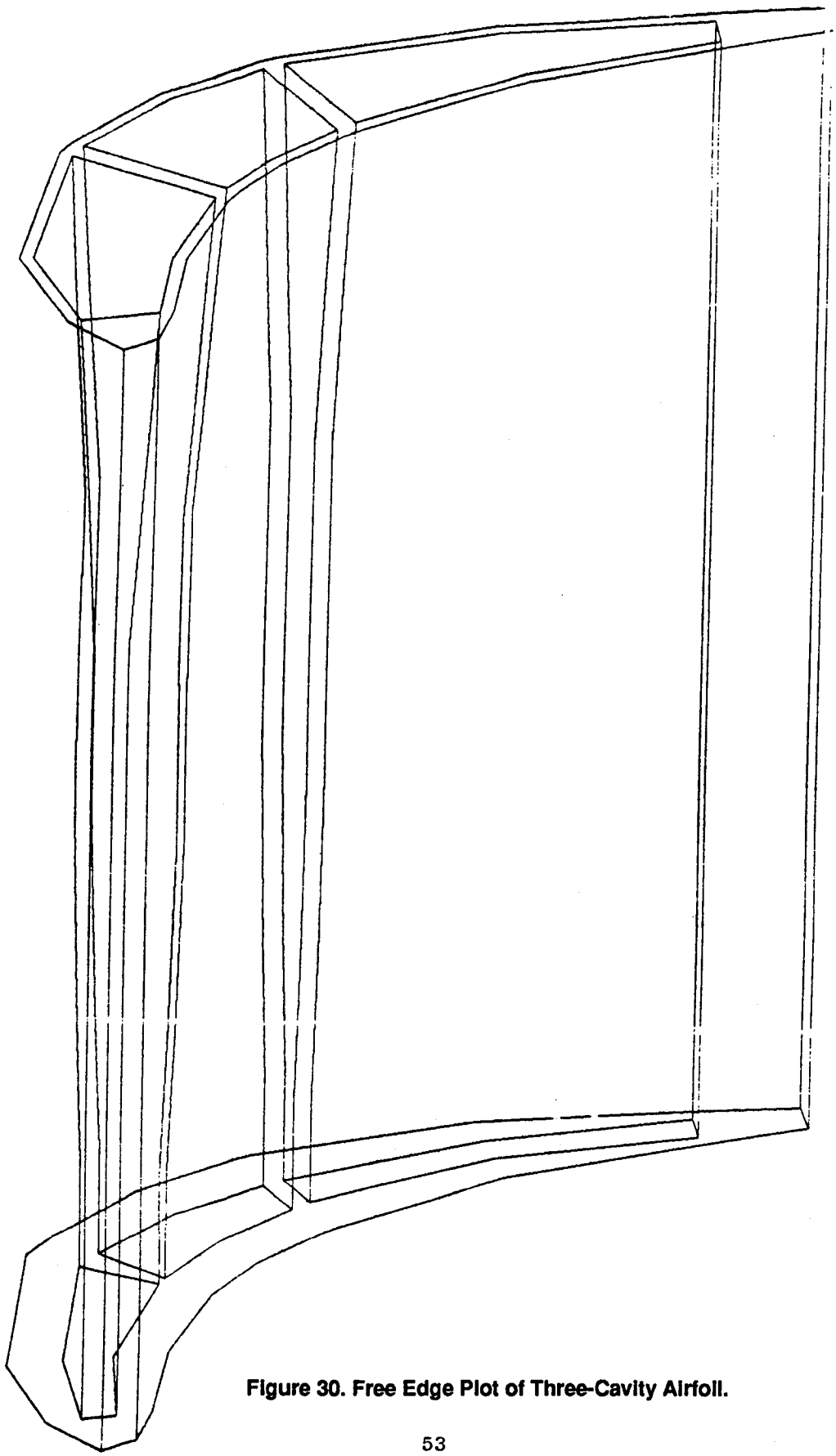

Figure 30. Free Edge Plot of Three-Cavity Airfoil.

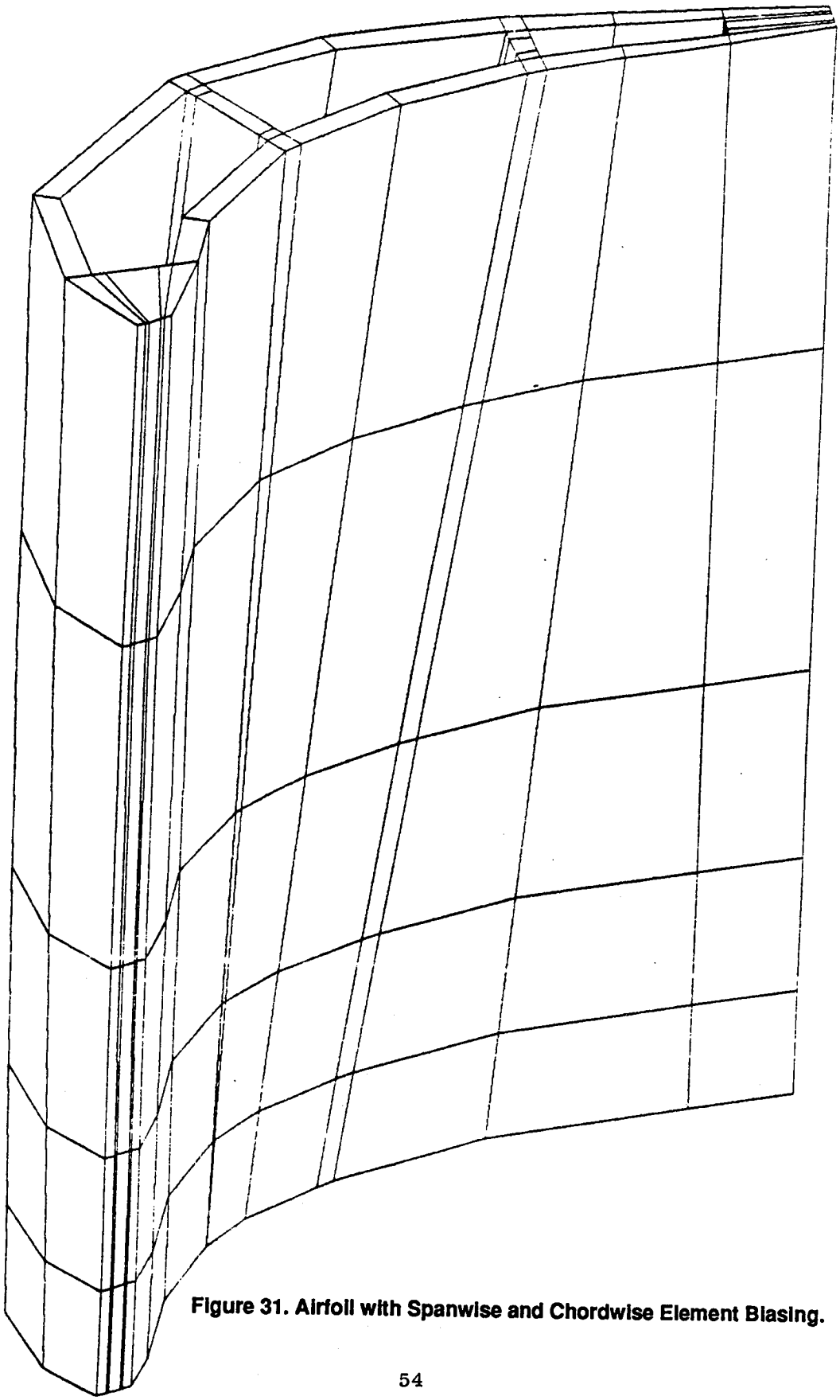

Figure 31. Airfoil with Spanwise and Chordwise Element Biasing.

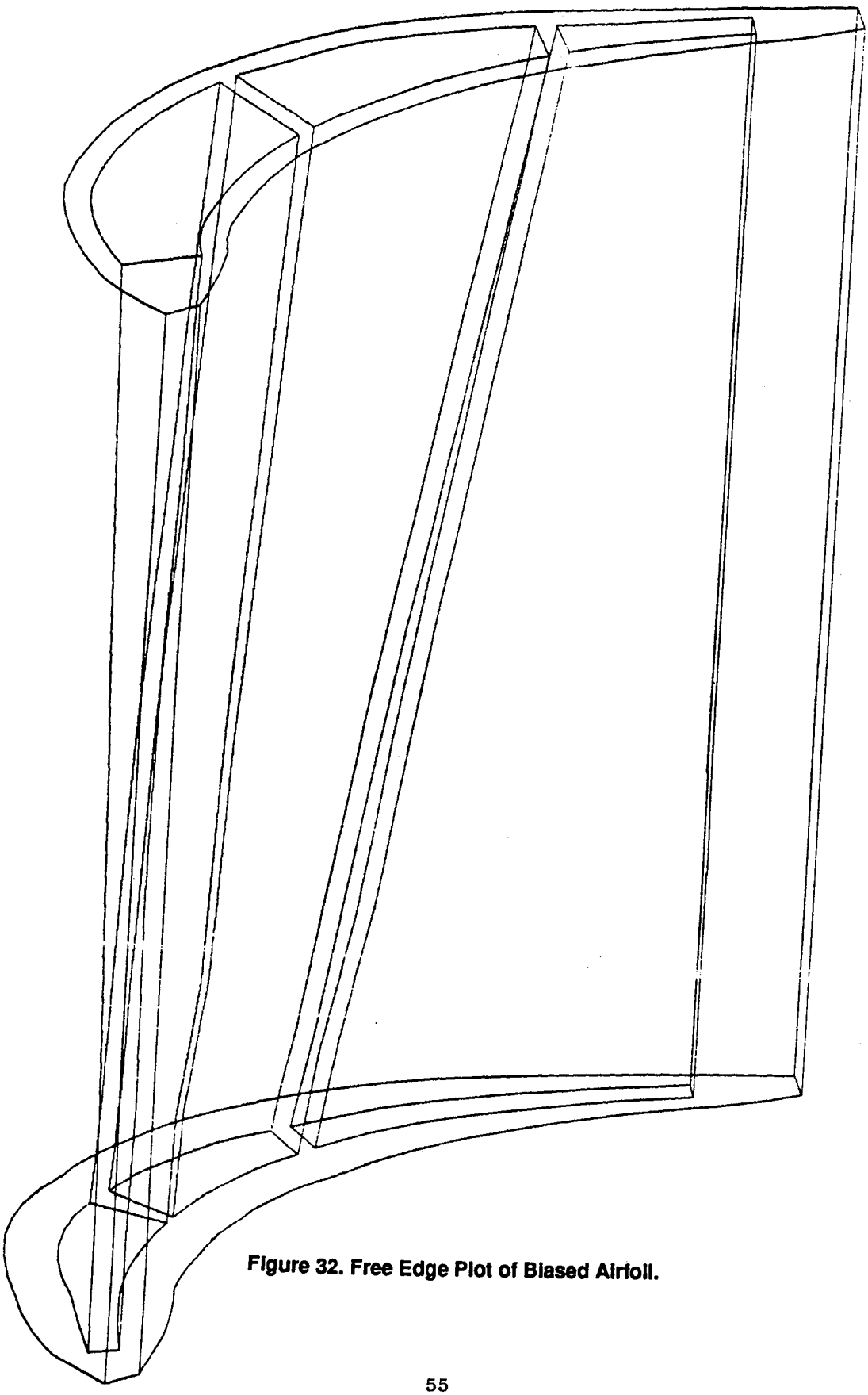

Figure 32. Free Edge Plot of Biased Airfoil.

2.8.2 Remeshing and Mesh Refinement

This area and the next, Self-Adaptive Solution strategies, touch on each other synergistically. What is sought in this program is the best combination of both. This involves two major areas of investigation: the method to be used to refine, upgrade, and rearrange the mesh, and the criteria to be used to activate this process.

There are a number of ways to refine a mesh to get a better answer: (1) one way is to progressively subdivide a coarse mesh, always retaining all previous meshes within the finer mesh; (2) a second family of techniques totally realigns the mesh based on some criteria such as strain energy density; (3) a third method is to leave the mesh unchanged but upgrade the order of the elements.

The first method, progressive subdivision, has certain theoretical and computational advantages. If the finite element interpolating functions used meet the requirements for completeness and continuity, convergence is mathematically guaranteed when we refine the mesh by progressive subdivision. The computational process of remeshing by progressive subdivision is straightforward; however, it guarantees a larger problem to solve.

For a solution of the finite element system of equations:

$$[K]\ \{\delta\} = \{F\}$$

suppose there is a numerical solution for the displacement, $\{\delta^*\}$. Then the equilibrium or residual force vector is generated:

$$\{R\} = \{F\} - [K]\ \{w^*\}$$

A perfect solution would result in this vector containing all zeros. Given the finite numerical accuracy of the computer, this is impossible. Therefore, a measure of the numerical "goodness" of the solution is to be found in how much this vector deviates from zero. Decisions on whether to re-solve or redefine the problem can be based on the total and local deviations from zero. If a few local degrees of freedom are out of equilibrium, this might suggest a local remeshing. If the total equilibrium is deficient, this will require remeshing and/or re-solving with greater numerical accuracy.

The decision tree for this is as follows

1. $\left.\begin{array}{l} \text{If } \Sigma R_i < C_R \\ \\ \text{and all } R_i < C_{R_{iL}} \end{array}\right\}$ the solution is good

2. If $\Sigma R_i > C_R$
   and [Number of nodes with $C_{R_{iL}} < R_i < C_{R_{iu}}$] $> C_s$
   then re-solve

3. If $\Sigma R_i > C_R$
   and [Number of nodes with $R_i > C_{R_{iu}}$] $< C_s$
   then remesh and re-solve

4. If $R_i < C_R$
   but some $R_i > C_{R_{iu}}$
   then remesh and re-solve

where:

R_i = i^{th} residual-free vector

$C_{R_{iL}}$ = Maximum allowable sum of R_i

$C_{R_{iu}}$ = Lower bound for Ri for possible remeshing

C_R = Maximum allowable upper bound for R_i

Once an acceptable displacement solution has been reached, proceed to the element level. If, at the elastic level, stresses and strains are linearly connected, only one of these two needs to be evaluated. Strain will be checked. The total strain at each calculation point in an element is made up of an elastic strain and a thermal strain:

$$\epsilon_i = \epsilon_i^e + \epsilon_i^\tau$$

One aspect of this program is the establishment of acceptable strain gradients for different element types. Between adjacent strain calculation points in one element, and probably over the entire element, a strain gradient would not be chosen that could encompass an elastic-plastic-elastic or a plastic-elastic-plastic variation. Therefore,

if

$$\epsilon_i^e - \epsilon_j^e \geq | 2\epsilon_{yield} |,$$

remesh this element.

Additionally, if the thermal strain changes in sign. Therefore,

if

$$\frac{\epsilon_i^\tau}{\epsilon_j^\tau} < 0$$

remesh this element.

Once the nonlinear solution has been entered, the element level checks become more complex and more important. The total strain is now made up of the elastic strain, thermal strain, plastic strain, and creep strain:

$$\epsilon_i = \epsilon_i^e + \epsilon_i^t + \epsilon_i^p + \epsilon_i^c$$

Now stress and strain are no longer linearly connected; stress is a function of elastic strain only. Once again, between any two adjacent calculation points within one element, an elastic strain gradient greater than the allowable material elastic gradient is not desirable. Thus,

if

$$\epsilon_i^e - \epsilon_j^e \geq | 2\epsilon_{yield} |,$$

remesh this element. The limit on the thermal strain would still be retained.

If

$$\frac{\varepsilon^{\tau}_{i}}{\varepsilon^{\tau}_{j}} < 0 \quad \text{, remesh this element.}$$

The next check is on the computed plastic and creep strain. No sign changes in either of these are allowed. In addition, a maximum gradient is set.

if

$$\frac{\varepsilon^{\rho}_{i}}{\varepsilon^{\rho}_{j}} < 0$$

or

$$\frac{\varepsilon^{c}_{i}}{\varepsilon^{c}_{j}} < 0$$

or

$$| \varepsilon^{\rho}_{i} - \varepsilon^{\rho}_{j} | > C_{P}$$

or

$$| \varepsilon^{c}_{i} - \varepsilon^{c}_{j} | > C_{C},$$

remesh this element.

Next, proceed to the interelement level check. These are of the same nature as the above, but now involve adjacent calculation points in adjacent elements.

2.8.3 Self-Adaptive Solution Strategies

In the development of basic self-adaptive solution strategies, we have used the work of Edward T. Wilson of the University of California at Berkeley, and Joseph Padovan and Surapong Tovichakchaikul of the University of Akron.

Wilson's efforts are directed toward an overall solution strategy, while Padovan's and Tovichakchaikul's work is on load incrementing and time-stepping for geometrical and material nonlinear solutions.

Wilson's philosophy on internal program organization for SAP-80 computer programs is applicable to the Component-Specific Modeling Program, with some extensions. He suggests that the basic internal organization of a computer program for structural analysis depends strongly on the method used to form and solve linear equations, with the frontal and profile (or active column) methods most often used. Both have the exact same economy so that the choice must be based on other factors.

In the frontal method, element stiffnesses and solutions of equations are formulated in a joint sequence manner. Therefore, all element stiffness subroutines, the equation solver, and the front of the stiffness matrix must be in core storage (or rolled in and out) during the reduction of the stiffness matrix. For the profile approach, the formation of all element stiffnesses for a particular type of element can be accomplished by a single call to one program segment. The formation of the total stiffness is a separate program segment in which the element stiffnesses are read in sequence from secondary storage and the total stiffness matrix is formed in active column blocks. In this case, the actual solution phase is another separate program link. Evaluation of substructure stiffnesses, calculations of mode shapes and frequencies, and evaluations of reactions and member forces are all separate links. This clear uncoupling of different phases of the program gives the profile approach a clear advantage in modularity and adaptive solution techniques. Also, the profile approach has no significant disadvantages when compared to the frontal method.

Padovan and his co-workers at the University of Akron have been developing "Self-Adaptive Incremental Newton-Raphson Algorithms" for nonlinear problems. They use a three-level approach. In the first level, incremental Newton-Raphson operators are used to "tunnel" into the problem solution space. The second level involves the constant monitoring of the different stages of solution through various quality/convergence/nonlinearity tests. The third level works with the results of the second level. The violation of any of the quality/convergences/nonlinearity tests triggers various scenarios for modifying the incremental Newton-Raphson strategy. The self-adaptive modifications triggered by the third level fall into one of three categories: global stiffness reformation; preferential, local reformation; or load increment adjustment. Recently, they have developed constrained, self-adaptive solution procedures for structures subject to high temperature elastic/plastic/creep effects. In this, they used closed, piecewise, continuous least-upper-bounding constraint surfaces that control the size of successive dependent variable excursions arising out of the time-stepping process.

A list of parameters to be controlled by the self-adaptive solution strategies has been generated. The parameters defined to date are listed below.

Parameters to be Controlled

1. Element Type(s)
2. Type(s) of Integration
3. Order(s) of Numerical Quadrature
4. Maximum Number of Iterations
5. Tolerance(s) on Convergence
6. Constitutive Equation(s)
7. Yield Criterion (Criteria)
8. Load Increments
9. Time Increments
10. Nonlinear Solution Algorithm(s)

Experience with the in-house programs has given us a good basis for developing the necessary tolerances on convergence. First, convergence is evaluated locally, not globally; that is, it is evaluated at each element or each numerical integration point. Second, for numerical conditioning, limits should be set below which inelastic strains are considered to be zero. Third, for time-dependent effects, both temperature and stress cutoffs should be established below which time dependent inelastic strain is considered to be zero. Then the local convergence criteria for incremental analysis are the following:

Time Independent

If

$$\varepsilon p < \text{PCUTOFF}, \ \varepsilon p \equiv 0.0$$

then

$$\Delta\varepsilon_{pI} < \text{TOL} = \text{CONVERGENCE}$$

or

$$\frac{\Delta\varepsilon pI - \Delta\varepsilon p\ (I-1)}{\Delta\varepsilon pI} < \text{TOL} = \text{CONVERGENCE}$$

Time Dependent

If

$$\text{TEMP} < \text{TOLC}, \ \varepsilon_c \equiv 0.0$$

and/or

$$\sigma_e < \sigma_c, \ \varepsilon_c \equiv 0.0$$

then

$$\Delta\sigma_{eI} < \text{CTOL} = \text{CONVERGENCE}$$

or

$$\frac{\Delta\sigma_{eI}\ \Delta\sigma_{e(I-1)}}{\Delta\sigma_{eI}} < \text{CTOL} = \text{CONVERGENCE}$$

The different convergence criteria are dictated by the wide material strength levels encountered in nonlinear analysis. We have also discovered that it is advantageous to be able to change these criteria during the course of an incremental analysis.

One approach taken in nonlinear computer codes is the right-hand-side technique, in which the plasticity is accounted for by adding an additional force vector to the right-hand side of the system of equations.

$$[K]\ \{d\} = \{F\} + \{f_p\}$$

The basic logic is as follows:

1. Solve for displacements from

   $$[K]\ \{d\} = \{F\} + \{f_p\}$$

2. Using the displacements and the constitutive equations, determine elastic and plastic strains for each element.

3. Check convergence.

4. Make an estimate of plastic strains that will satisfy the constitutive equations, equilibrium, and compatibility.

5. Based on the estimate of plastic strains from Step 4, form a new plastic load vector and go back to Step 1.

This iteration scheme continues until the convergence criteria are satisfied.

The plastic iteration accounts for a considerable portion of the total computer cost in running a nonlinear finite element code. Substantial improvements have been made in accelerating the convergence of plastic iteration by improving the estimate of the solution in Step 4. Three options are now available.

The first of these schemes is the simplest, and uses the current calculation of plastic strain from the constitutive equations as the estimate of the solution. This is the usual method on right-hand-side iteration schemes.

The second scheme is a modification of the original iteration scheme, and is essentially a successive-over-relaxation (SOR) scheme. The estimate of the solution is given by:

$$\hat{\epsilon}_p^i = \epsilon_p^{i-1} + \alpha \left(\epsilon_p^i - \epsilon_p^{i-1} \right)$$

$\hat{\epsilon}_p^i$ = current estimate of solution

ϵ_p^{i-1} = previous calculation of plastic strain from constitutive equations

ϵ_p^i = current calculation of plastic strain from constitutive equations

α = current acceleration factor

α = 1.5 is used

This estimation procedure continues until $\varepsilon_p^i < \varepsilon_p^{i-1}$, then the following is used:

$$\varepsilon^i = \varepsilon^{i-1} + 0.5 \quad \varepsilon_p^i - \varepsilon^{i-1}$$

The third scheme is based on an Aitken's extrapolation formula for a fixed-point iteration. Although we are not really doing a fixed-point iteration, the finite element equations behave in much the same way. The equation used in estimating the solution is:

$$\hat{\varepsilon}_p^i = \varepsilon_p^{i-2} - \frac{\left(\varepsilon_p^{i-1} - \varepsilon_p^{i-2}\right)^2}{\varepsilon_p^i + 2\varepsilon_p^{i-1} + \varepsilon_p^{1-2}}$$

Where the symbols are as before and ε_p^{i-2} = calculation of plastic strain from the constitutive equations two iterations ago.

The Aitken's extrapolation works best when performed every third iteration. In between Aitken's extrapolations

$$\hat{\varepsilon}_p^i = \varepsilon_p^i$$

2.8.4 COSMO SYSTEM FOR COMBUSTOR NUGGETS

Figure 33 shows a flow chart of the overall COSMO system including the action positions of the adaptive controls developed in this program. For the combustor, the following adaptive controls have been incorporated into the system (the numbers are consistent with Figure 33).

1. time increment
2. load increment
3. plasticity tolerances
4. creep tolerances
5. number of master region elements
6. number of slices
7. position of slices
8. row refinement
9. element refinement

The first four adaptive controls are a function of the structural code being used. For this system the code and the controls are those developed under "3D Inelastic Analysis Methods for Hot Section Structures." The other adaptive controls are keyed from a decision grid as indicated in Figure 34. The gradients in normalized stress, total strain, plastic strain, and creep strain will be used to rank requirements.

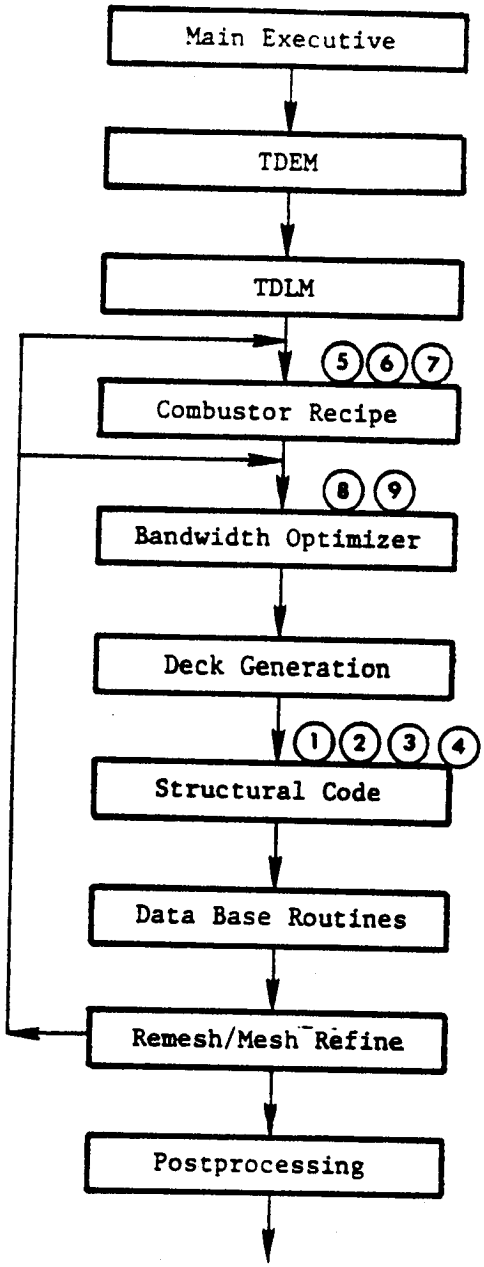

Figure 33. System Flow Chart Showing Adaptive Control Positions.

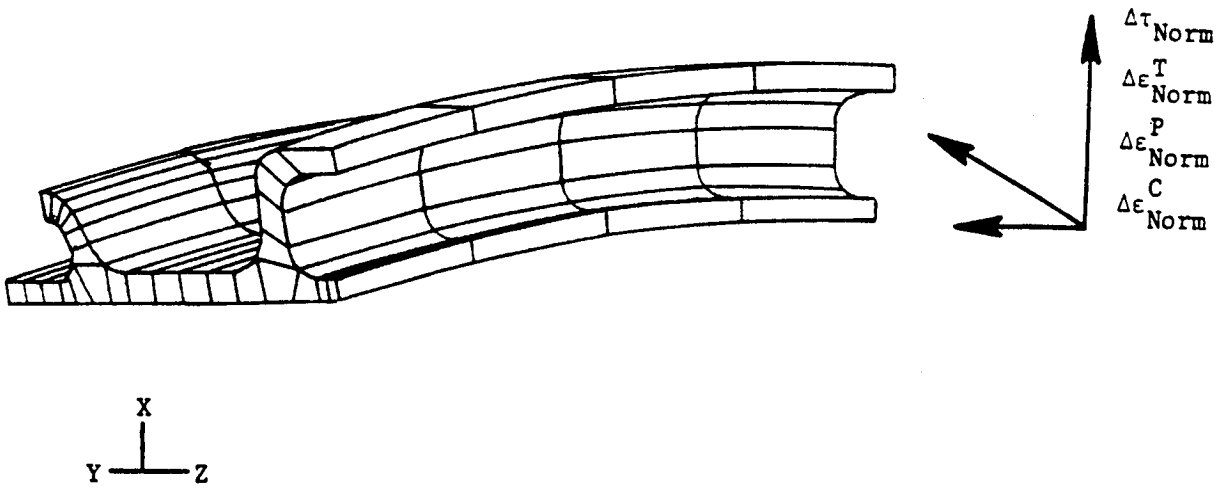

Figure 34. Combustor Nugget Decision Grid.

3.0 EXECUTIVE SUMMARY

The objective of this program has been to develop and verify a system of interdisciplinary modeling and analysis techniques specific to three hot section components of gas turbine engines. These techniques incorporate data and theoretical methods from cycle and performance analysis, heat transfer analysis, linear and nonlinear stress analysis, and mission analysis. Combining and expanding on proven techniques, this program provides an integrated system for accurate and efficient prediction of temperature, deformation, stress and strain histories throughout a complete flight mission. The system is specialized for combustor liners, hollow, air-cooled turbine vanes, and turbine blades.

Performance of the program was accomplished in two parallel work efforts as depicted in Figure 1. A Structural Modeling effort included evaluation of existing analysis methods, design of software to implement the chosen methods, and development of geometric modeling and structural analysis capabilities.

The second work effort involved development of a thermodynamic engine model, a thermomechanical load mission model, and a mission model decomposition and synthesis capability.

4.0 REFERENCES

1. McKnight, R. L., "Component Specific Modeling - First Annual Status Report," NASA CR-174765, 1983.

2. McKnight, R. L., "Component Specific Modeling - Second Annual Status Report," NASA CR-174925, 1985.

APPENDIX A

TASK II - DESIGN OF STRUCTURAL ANALYSIS SOFTWARE ARCHITECTURE

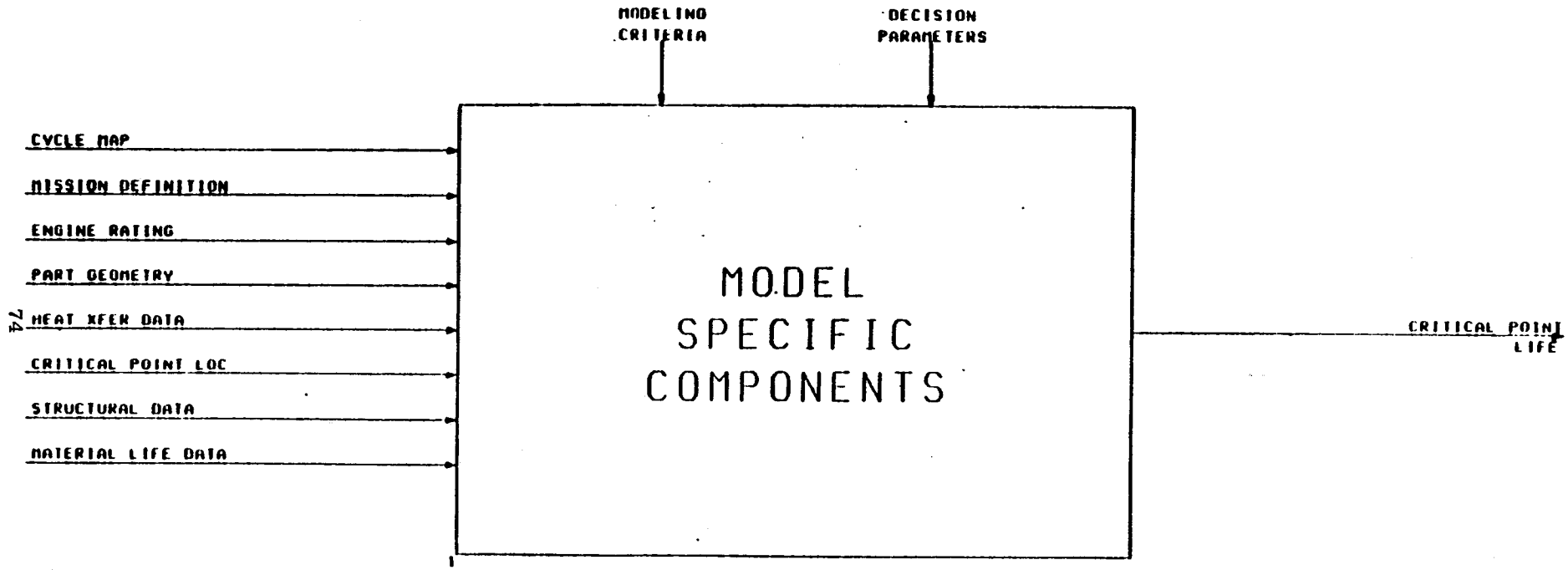

COSMOS - CONTEXT

A-0

REVISION- 4

8 10 83

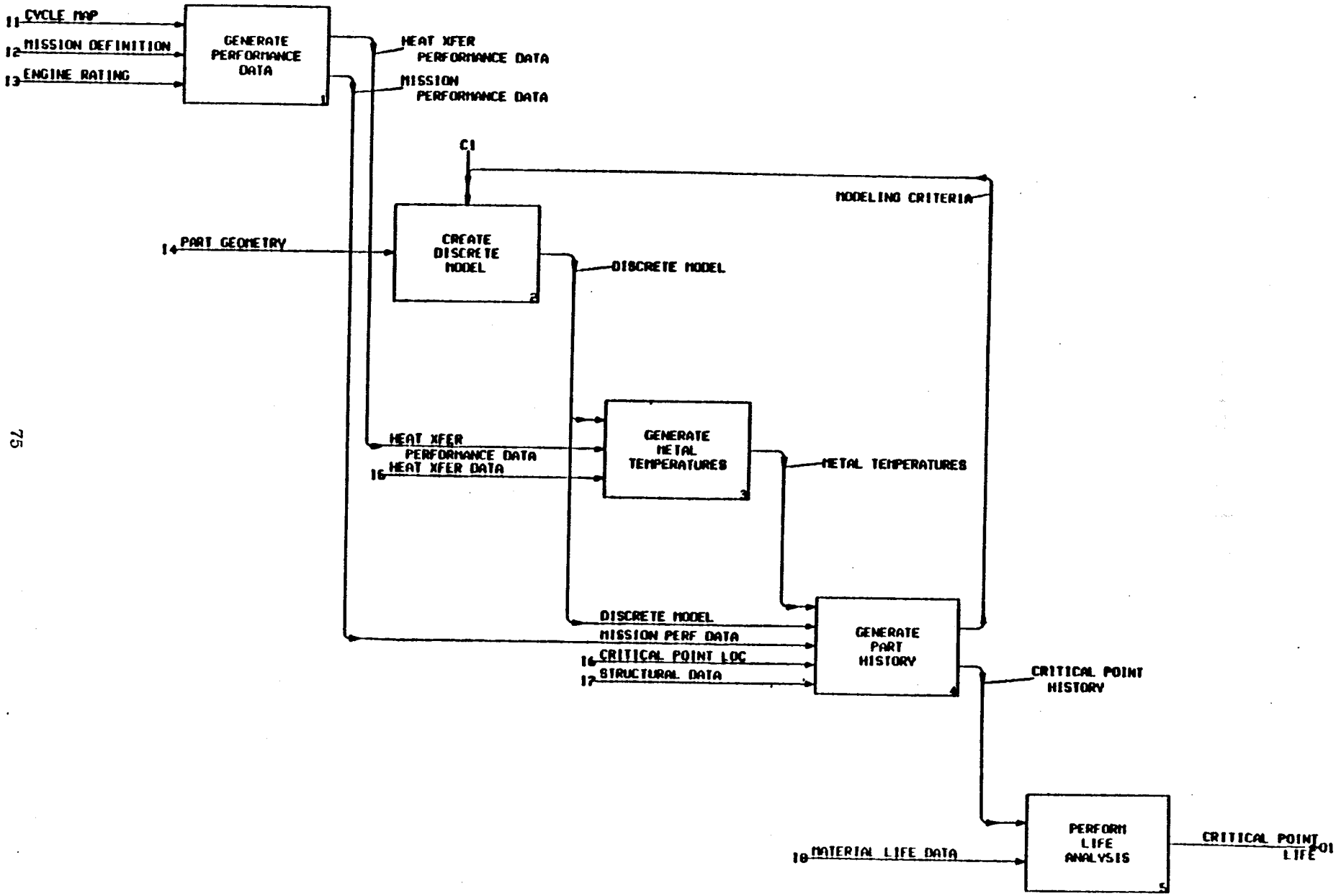

Model Specific Component

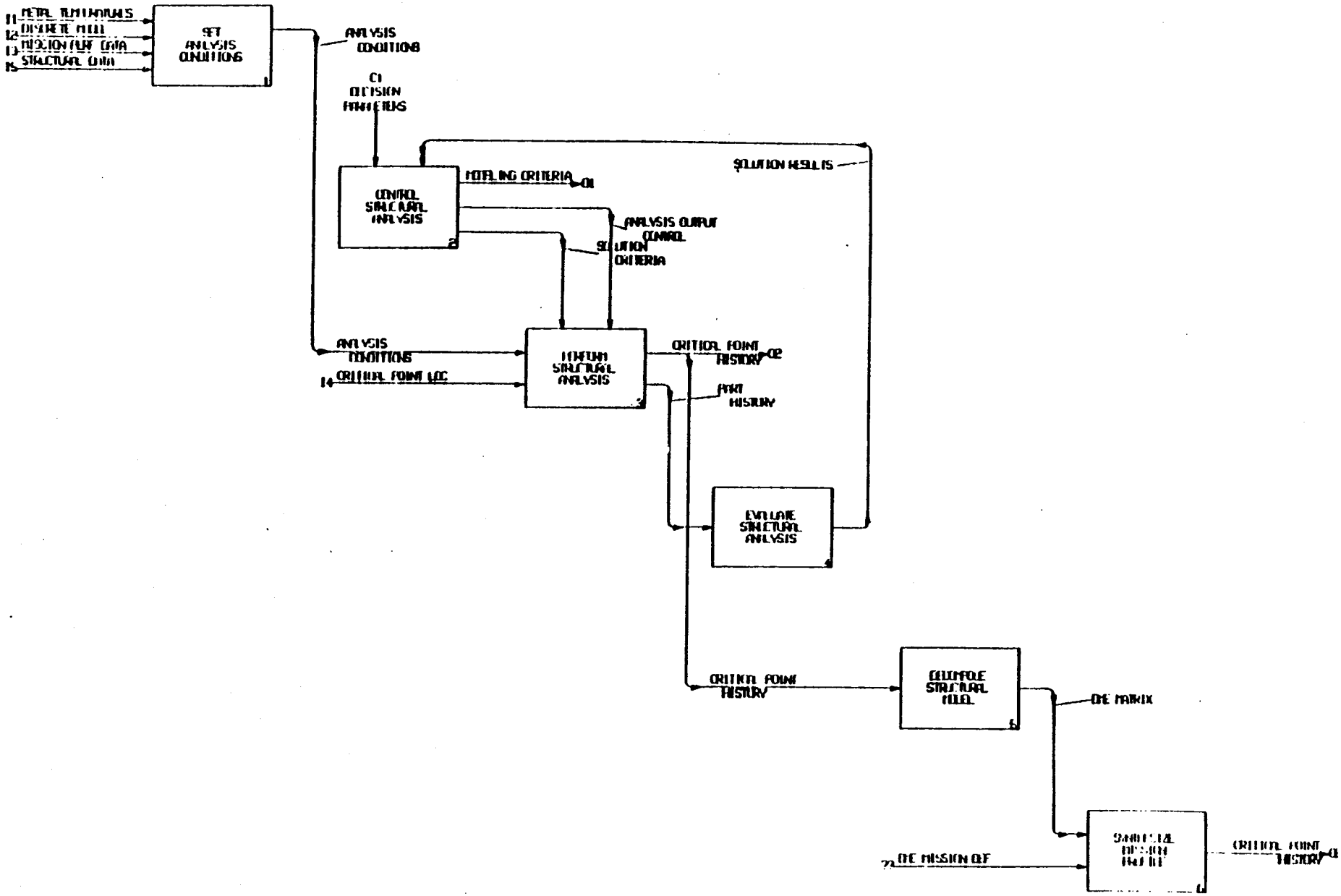

GENERATE PART HISTORY

A4

REVISION 1

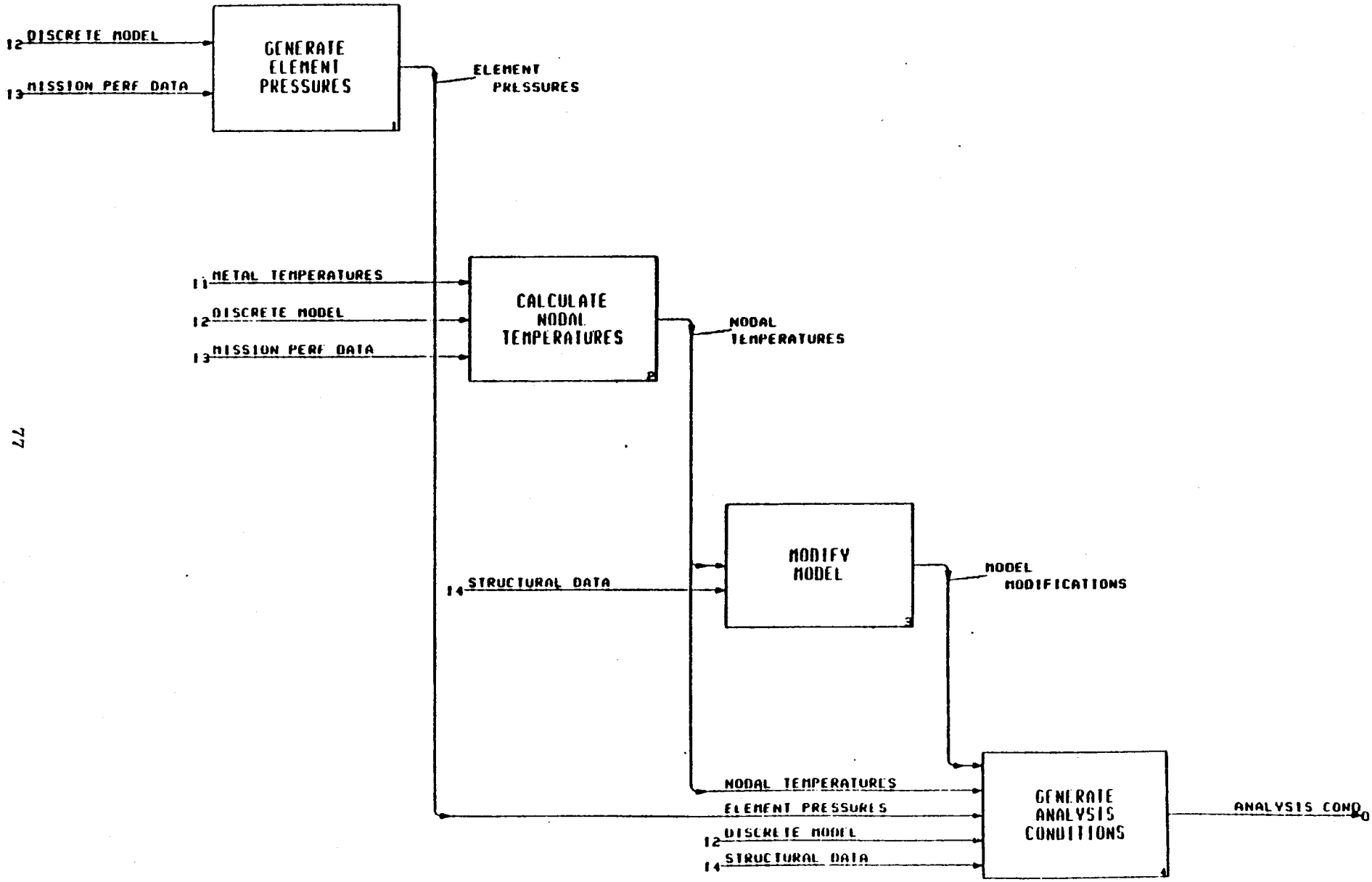

77

SET ANALYSIS CONDITIONS

A4.1

REVISION- 1

8-10-83

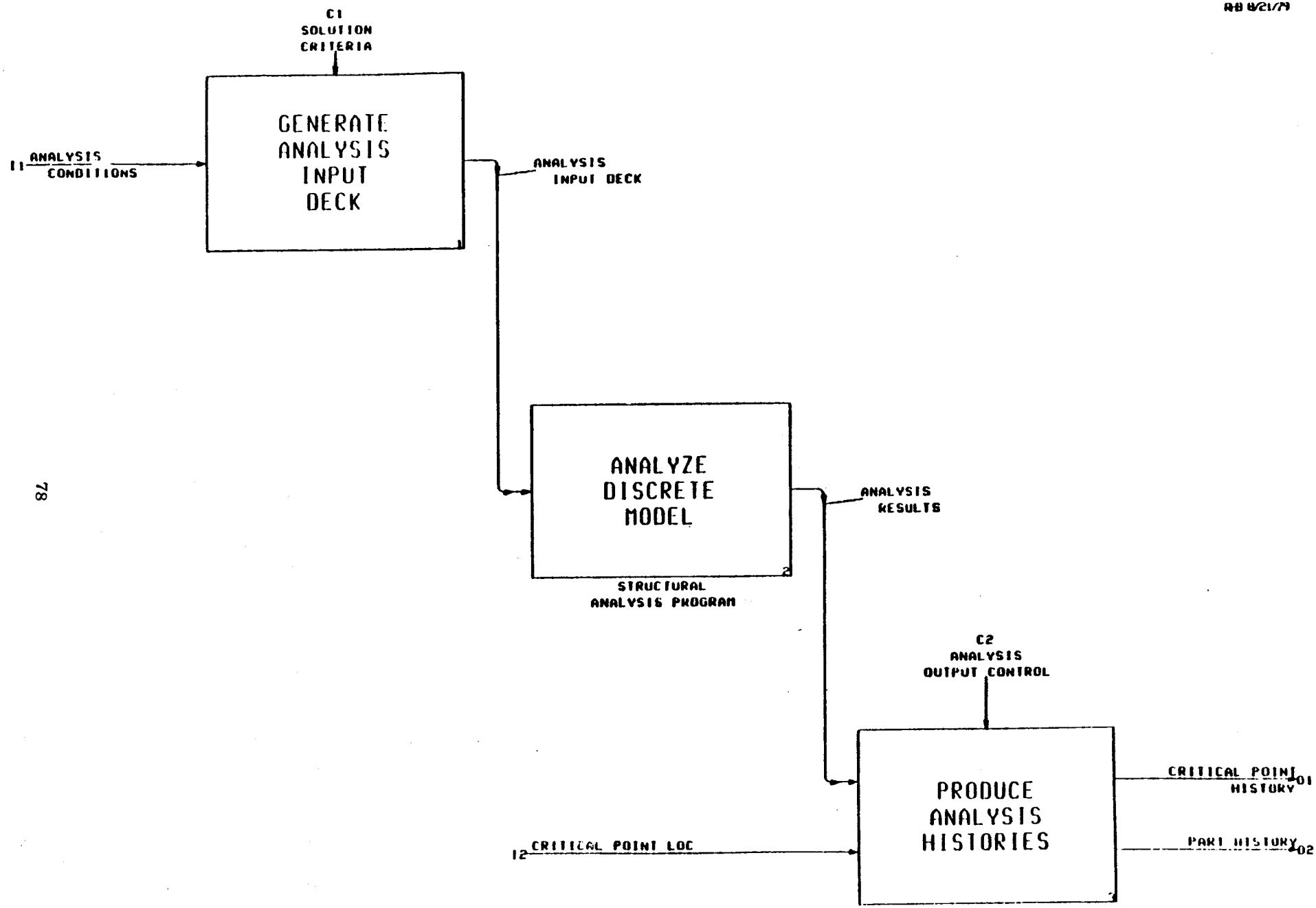

78

PERFORM STRUCTURAL ANALYSIS

A4.3

REVISION- 1

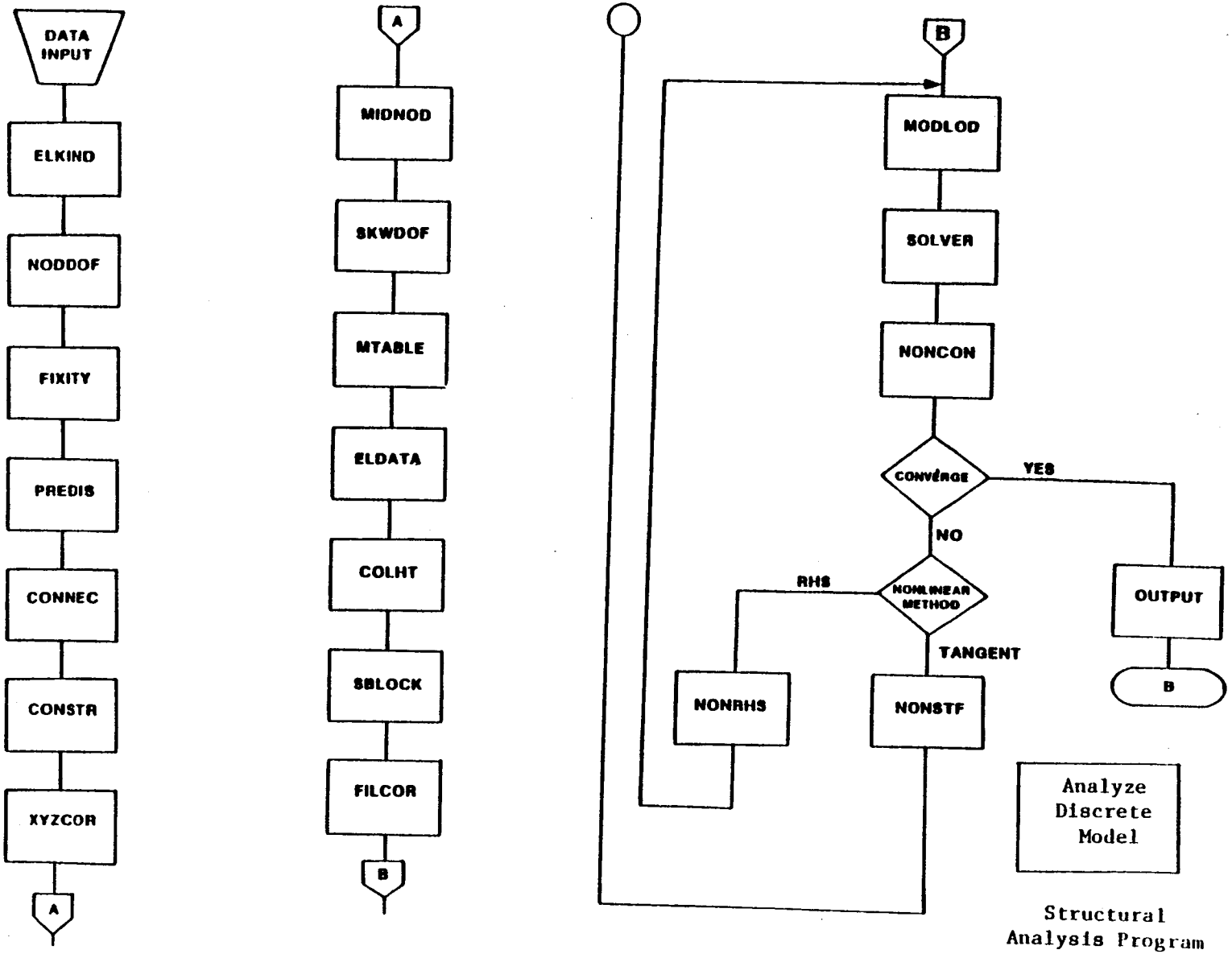

Structural Analysis Program

PREPROCESSOR ATTRIBUTES:

A. SOFTWARE

- Modular in Structure
- Machine Independent
- Low Core Requirement
- Extensive Documentation

B. FEATURES/OPERATION

- User Friendly
- Extensive Diagnostics
- Complete Data Summary
- Interactive Graphics
  - Model Geometry
  - Material Physical Properties

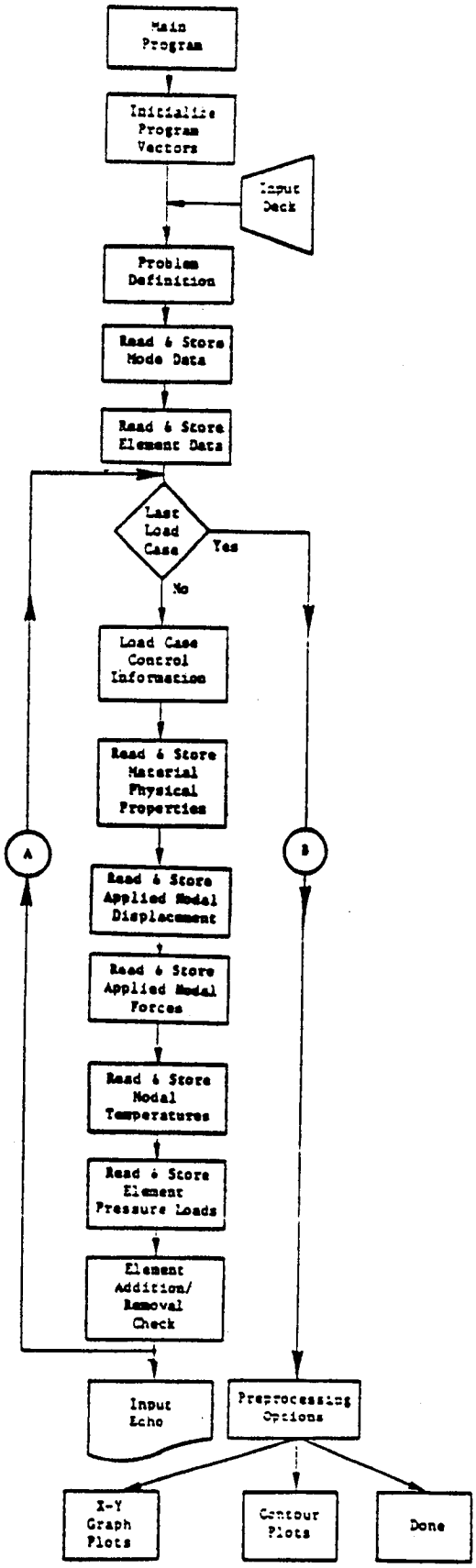
Main Program
Initialize Program Vectors
Input Deck
Problem Definition
Read & Store Mode Data
Read & Store Element Data
Last Load Case
Yes
No
Load Case Control Information
Read & Store Material Physical Properties
Read & Store Applied Modal Displacement
Read & Store Applied Modal Forces
Read & Store Modal Temperatures
Read & Store Element Pressure Loads
Element Addition/ Removal Check
A
B
Input Echo
Preprocessing Options
X-Y Graph Plots
Contour Plots
Done

POSTPROCESSOR ATTRIBUTES:

A. SOFTWARE

- Modular in Structure
- Machine Independent
- Low Core Requirement
- Extensive Documentation

B. FEATURES/OPERATION

- User Friendly
- Will Function in Batch or Time-Share Environment
- Will Have Extensive Graphics Capabilities
  - X-Y Graph Plots
  - Contour and Deflected Shape Plots at Defined Planes
- Will Have Built-in Data Manipulation Routines (User Controlled)
  - User Friendly Data Base

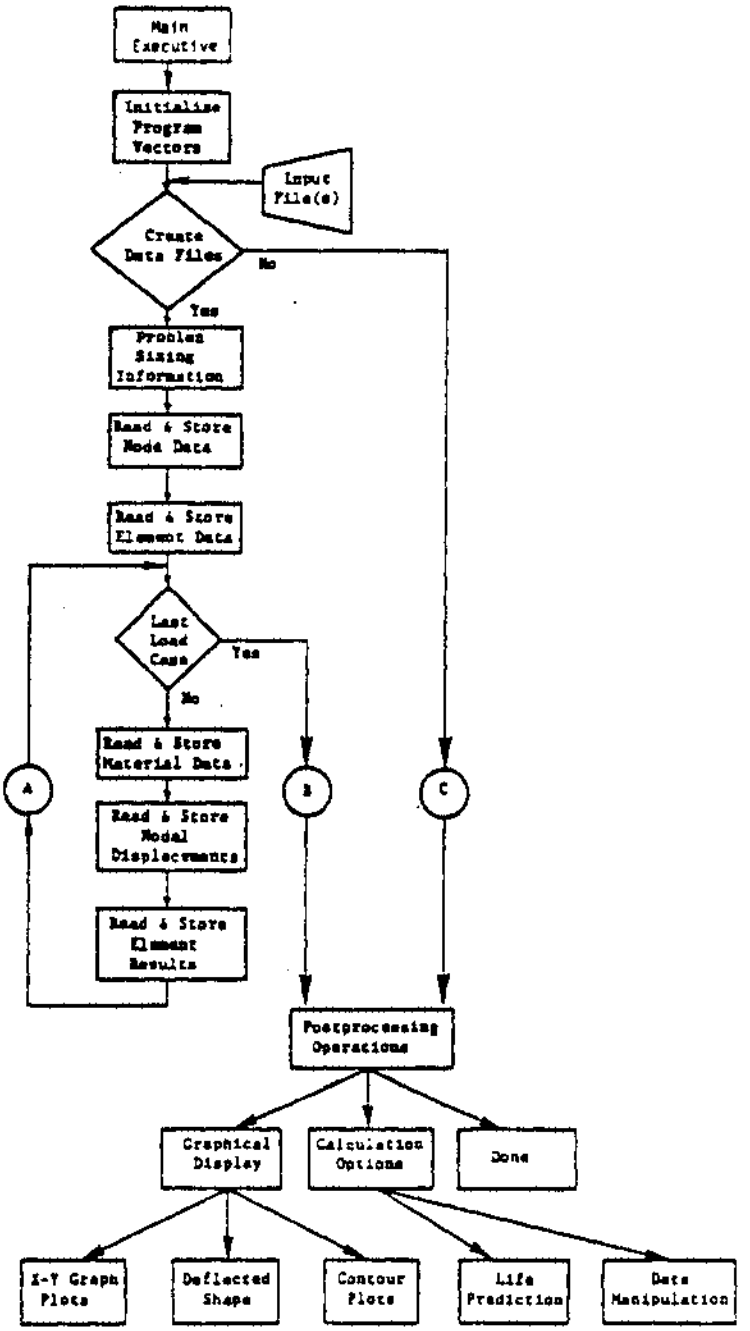
Main Executive
Initialise Program Vectors
Input File(s)
Create Data Files
No
Yes
Problem Sizing Information
Read & Store Node Data
Read & Store Element Data
Last Load Case
Yes
No
Read & Store Material Data
Read & Store Nodal Displacements
Read & Store Element Results
A
B
C
Postprocessing Operations
Graphical Display
Calculation Options
Done
X-Y Graph Plots
Deflected Shape
Contour Plots
Life Prediction
Data Manipulation

APPENDIX B

COMPONENT TEMPERATURE AND PRESSURE DECOMPOSITION AND SYNTHESIS PLAN

I. Blades and Vanes

A. Input will be:

1. A series of mid-span station temperatures at a specified SS reference case condition, and for each station a percent cord envelope dimension.
2. A set of output percent cord envelope dimensions.
3. A table of percent radial span (or radii) versus temperature factors, RF, where:

$$RF = \frac{Ts-T3}{Tms-T2}$$

Ts = temperature at specified span dim.

Tms = temperature at midspan.

The point density in this table will be such that spanwise linear interpolation will suffice.

B. Calculations

1. For each temperature a nominal cooling effectiveness will be calculated from:

$$\eta_c = \frac{T41-Tm}{T41-T3}$$

2. At each new condition, all station η_c values will be modified by a factor, CF, as follows:

$$CF = \frac{(1-\eta_c)}{(1-\eta_c)REF} = (T3*T41)^{\alpha}/(T3*T41)^{\alpha}_{REF}$$ where α is input

3. Output Nc values will be linearly interpolated based on percent cord envelope at adjacent input stations.
4. For each output radial distance (specified in the input) all station temperatures will be calculated as follows:

$$Tij = T3 + (1-\eta_{c_R})*CF(T41-T3)*RF$$

Where i = station index
j = radial station index

II. Combustor

A. Inputs will be:

1. Metal bulk made temperatures at axial stations on inner and outer liners, and for each station, x and y dimensions of node centers at a specified reference case condition. Both hot streak and average metal temperature values will be input.
2. It is assumed that output node dimensions will match the input nodes. If cross-meshing is to be required, it will be done before the input is defined.
3. A set of linear equation constants will be input for a sparse set of axial locations, identified by ΔT station: numbers. Output ΔT locations will be same as input locations.
4. A set of ΔP scaling constants will be input at a sparse set of locations, identified by ΔP station numbers. Output ΔP stations will be same as input.

B. Calculations

1. A nominal cooling effectiveness will be calculated for each input combustor average and hot streak temperature.
2. At each flight condition, each metal temperature will be recalculated from:

$$Tm_{ij} = T3_j + (1-\eta_{c_i})(T41_j-T3_j)$$

Where i = station index
j = flight phase index

3. At each flight condition, each ΔT will be recalculated from:

$$\Delta T_{ij} = [(1-\eta_{c_i})*T41_j + (\eta_{c_i}-1)*T3_j] \quad [b_i+m_i*P3_j]$$

4. At each flight condition, each ΔP will be recalculated from:

$$\Delta P_{ij} = P3_j*K_i*\frac{W41}{P3}^2_j * T3_j$$

APPENDIX C

THERMODYNAMIC ENGINE MODEL SPECIFICATION

I. Input

A. Setup information (furnished with model)
   1. Engine performance data; 148 cases per Table I-A-1.
      a. Case parameters per Table I-A-1-a.
   2. Engine rating data - Table I-A-2.1-3.
   3. Power level index matrix, Table I-A-3.

B. User Information
   1. Mission definition data
      a. One line for each mission phase point.
      b. Each line contains the following control data:
         1. Phase #
         2. Mach number
         3. Altitude - feet
         4. Offset from standard day - °F
         5. Power level parameter code #
         6. Power level parameter value
         7. Customer bleed - #/sec.
         8. Deterioration level - °F
         9. Time increment between this phase point and the next, min.
      c. One line, following the mission phase point data line, for each parameter to be offset from its steady state value.
      d. Each offset line shall contain:
         1. Phase #
         2. Parameter #
         3. Offset factor
         4. Offset adder

II. Output

A. A performance case for each mission phase point
   1. Parameters per Table I-A-1-a.
   2. Format similar to Table II-A-2.

III. Technical Basis

A. Each new case will be generated from available cases (I-A-1) by a disciplined interpolation process similar to that currently used in the Life Analysis by Stress and Temperature Simulation (LASTS) program.
   1. All parameters will be transformed to a functional form that has optimal linearity relative to all other parameters.
      a. A study will be performed on CF6-50C2 engine performance data to evaluate and improve the interpolation functions.

III. A. 2. Each transformed parameter will be interpolated by a linear interpolation process and then transformed back to its normal form.

3. The interpolation "targets" shall be specified in the input for each mission phase point (I-B-1-b).

4. The interpolation process for each phase point shall begin with a base case near the desired mission phase point.

5. Each interpolation step will convert the base case (or previously modified case) to the desired level of the target control parameter (i.e., MN).

a. Linear partials are assumed; interactions are ignored.

b. Partials will be derived from two or more "partial cases" near the base case conditions.

c. The interpolation steps will be performed in the sequence in Table I-A-1-a.

d. The specific power level parameter to be used as an interpolation target is input as "power level #", followed by the target value.

e. For flight idle and ground idle, a special power level # (one for FI or one for GI) will be entered, followed by a zero parameter value; the standard FI and GI power levels will be used.

f. For thrust reverse, a special power level # will be used and a value of fan speed will follow; thus thrust reverse power level will always be based on a fan speed target.

B. The LASTS interpolation process will be modified to eliminate the current manual procedure for the generation of interpolation instructions.

1. A set of base case numbers will be provided as a function of altitude and Mach number.

2. A family of pairs or triplets of partials case numbers will be provided as a function of altitude and Mach number for each control parameter.

3. The user will be required to input only the data in I-B-1-b for each mission phase point.

C. The Thermodynamic Engine Model (TDE) shall have the capability to predict the minimum time for speed changes due to throttle actions.

1. The user shall have the option to input zero throttle-action transient times, and the model will calculate appropriate transient times, subtracting them from following phase times.

2. The transient time calculation shall be sensitive to the effects of altitude.

D. The user shall have the option of selecting an appropriate CF6-50C2 power management point, and avoid the need for specifying absolute values of the power level parameter.

1. The power management parameter code shall call for take-off, max climb, or max cruise rating, and the adjacent value shall specify the % derate desired based on % thrust.

III. E. Offsets of specific parameters, relative to the steady state performance cases shall be permitted to simulate take-off transient conditions.

1. Each parameter change shall be specified by a line following the mission phase point data.
2. The parameter offset data shall be:
   a. Case #
   b. Parameter #
   c. Offset factor
   d. Offset adder
3. Offset calculations will be performed after mission phase point interpolations are completed.

IV. Software Characteristics/Interfaces

A. Later (to be integrated with overall software of the COSMOS Program).

TABLE I-A-1
CF6-50C2 PERFORMANCE CASES

	M	A	PCNLR	PCNHR2	ΔTo	OFFSETS WB	DT49 °F
1	0	0	109		0	N	50
2			100				
3			90				
4			75				
5			55				
6				FI			
7				GI			
8	0	0	109		-30	N	50
9			100				
10			90				
11			75				
12			55				
13				FI			
14				GI			
15	0	0	109		+30	N	50
16			100				
17			90				
18			75				
19			55				
20				FI			
21				GI			
22	0	0	109		0	0	50
23			100				
24			90				
25			75				
26			55				
27				FI			
28				GI			
29	0	0	109		0	N	0
30			100				
31			90				
32			75				
33			55				
34				FI			
35				GI			
36	4	5	114		0	N	50
37			104.5				
38			94				
39			78				
40			57				
41				FI			
42				GI			

	M	A	PCNLR	PCNHR2	ΔTo	OFFSETS WB	DT49 °F	
43	.4	5	114		18	N	50	
44			104.5					
45			94					
46			78					
47			57					
48				FI				
49				GI				
50	.4	5	114		0	0	50	
51			104.5					
52			94					
53			78					
54			57					
55				FI				
56				GI				
57	.4	5	114		0	N	0	
58			104.5					
59			94					
60			78					
61			57					
62				FI				
63				GI				
64	0	5	114		0	N	50	
65			104.5					
66			94					
67			78					
68			57					
69				FI				
70				GI				
71	.4	0	109		0	N	50	
72			100					
73			90					
74			75					
75			55					
76				FI				
77				GI				
78	.18	0	109		0	N	50	T/R
79			100					
80			90					
81			75					
82			55					
83	.4	15	106		0	N	50	
84			94					
85			77					
86			59					
87				FI				
88				GI				
89	.65	15	106		0	N	50	
90			94					

TABLE I-A-1
CF6-50C2 PERFORMANCE CASES

	M	A	PCNLR	PCNER2	ΔTo	OFFSETS WB	DT49 °F
91	.65	15	77		0	N	50
92			59				
93				FI			
94				GI			
95	.65	15	106		18	N	50
96			94				
97			77				
98			59				
99				FI			
100				GI			
101	.65	15	106		0	0	50
102			94				
103			77				
104			59				
105				FI			
106				GI			
107	.65	15	106		0	N	0
108			94				
109			77				
110			59				
111				FI			
112				GI			
113	.65	35	117		0	N	50
114			104				
115			84				
116			65				
117				FI			
118				GI			
119	.8	15	106		0	N	50
120			94				
121			77				
122			59				
123				FI			
124				GI			
125	.8	35	117		0	N	50
126			104				
127			84				
128			65				
129				FI			
130				GI			
131	.8	35	117		18	N	50
132			104				
133			84				
134			65				
135				FI			
136				GI			
137	.8	35	117		0	0	50
138			104				

TABLE I-A-1
CF6-50C2 PERFORMANCE CASES

	M	A	PCNLR	PCNHR2	ΔTo	OFFSETS WB	DT49 °F
139	.8	35	84		0	0	50
140			65				
141				FI			
142				GI			
143	.8	35	117		0	N	0
144			104				
145			84				
146			65				
147				FI			
148				GI			

TABLE I-A-1a
ENGINE PERFORMANCE CASE PARAMETERS

P2	Fan Inlet Total Pressure	PSIA
P3	Compressor Discharge Total Pressure	PSIA
P4	Turbine Inlet Total Pressure	PSIA
P49	Turbine Outlet Total Pressure	PSIA
T2	Fan Inlet Total Temperature	°F
T3	Compressor Discharge Total Temperature	°F
T41	Turbine Inlet Total Temperature	°F
T49	Turbine Outlet Total Temperature	°F
W25	Fan Air Flow	#/sec
FNIN1	Installed Thrust	#
DTAMB	Offset from Standard Day Temperature	°F
W41	Turbine Air Flow	#/sec
XNH	Core Speed	RPM
XNL	Fan Speed	RPM
MN	Mach Number	
ALT	Altitude	Feet
WB27/WB3	Customer Bleed	#/sec
DT49	Engine Deterioration Index	°F

TABLE I-A-2.1
APPROX. CF6-50C2 RATING DATA

TAKEOFF

°C T2	Feet ALT	PCNLR	XNLR	ALT	PCNLR	XNLR	ALT	PCNLR	XNLR
-60	0	107.75	3736	1000	110.4	3789	2000	111.1	3814
20									
23									
25.5									
27									
28.5								110.4	3789
30.5					109.75	3767		109.75	3767
50		105.7	3628		105.7	3628		105.7	3628
60		97.8	3357		97.8	3357		97.8	3357

T2	ALT	PCNLR	XNLR	ALT	PCNLR	XNLR	ALT	PCNLR	XNLR
-60	3000	111.85	3839	4000	112.75	3870	≥ 5000	113.82	3907
20									
23								112.75	3870
25.5					111.85	3839		111.85	3839
27		111.1	3814		111.1	3814		111.1	3814
28.5		110.4	3789		110.4	3789		110.4	3789
30.5		109.75	3767		109.75	3767		109.75	3767
50		105.7	3628		105.7	3628		105.7	3628
60		97.8	3357		97.8	3357		97.8	3357

TABLE I-A-2.2
APPROX. CF6-50C2 RATING DATA

MAX CLIMB

^{o}C T2	FEET ALT	PCNLR	XNLR	FEET ALT	PCNLR	XNLR	FEET ALT	PCNLR	XNLR
-60.0	36089	117.1	4019	42000	116.2	3989	30000	113.6	3899
-7.0									
-5.7		116.2	3989						
-1.2		113.6	3899		113.6	3899			
11.0		106.7	3662		106.7	3662		106.7	3662
21.2		103.4	3549		103.4	3549		103.4	3549
34.0		98.5	3381		98.5	3381		98.5	3381
60.0		90.4	3103		90.4	3103		90.4	3103

T2	ALT	PCNLR	XNLR	ALT	PCNLR	XNLR	ALT	PCNLR	XNLR
-60.0	20000	106.7	3662	10000	103.4	3549		98.5	3381
-7.0									
-5.7									
-1.2									
11.0									
21.2		103.4	3549						
34.0		98.5	3381		98.5	3381			
60.0		90.4	3103		90.4	3103		90.4	3103

TABLE I-A-2.3
APPROX. CF6-50C2 RATING DATA

MAX CRUISE

°C T2	FEET ALT	PCNLR	XNLR	FEET ALT	PCNLR	XNLR	FEET ALT	PCNLR	XNLR
-4.5	36089	112.42		30000	109.70		42000	109.25	
-1.0		109.70							
0		109.25			109.25				
9.2		104.45			104.45			104.45	
+20		100.64			100.64			100.64	
+29.2		97.47			97.47			97.47	
+43.7		92.70			92.70			92.70	
+60.0		87.35			87.35			87.35	

T2	ALT	PCNLR	XNLR	ALT	PCNLR	XNLR	ALT	PCNLR	XNLR
-4.5	25000	104.45		20000	100.64		10000	97.47	
-1.0									
0									
9.2									
20.0		100.64							
29.2		97.47			97.47				
43.7		92.70			92.70			92.70	
60.0		87.35			87.35			87.35	

T2	ALT	PCNLR	XNLR
-4.5	0	92.70	
-1.0			
0			
9.2			
20.0			
29.2			
43.7			
60.0		87.35	

TABLE I-A-3

AUTOMATED INTERPOLATION SYSTEM

POWER LEVEL INDEX

CF6-50C2

	PCNLR	
P.L. INDEX	ALT 0	ALT 10000'
1	109.0	119.0
2	100.0	109.0
3	90.0	98.0
4	75.0	81.0
5	55.0	58.0
6	38.0	44.0
7	24.0	34.0

P.L. INDEX	ALT 10000'	ALT 40000'
1	103.5	120.0
2	91.5	106.0
3	75.0	85.0
4	58.0	67.0
5	44.0	48.0
6	34.0	37.0

TABLE II-A-2

PERFORMANCE DATA OUTPUT FORMAT

* ENGINE PERFORMANCE DATA BY MISSION PHASE *

PHASE #	CASE #	** ENGINE PARAMETER ** P48	PS	W25	FNIN1	DTAMB
1	197	14.476	14.476	1.108	0.	1.700
2	190	14.476	14.476	1.108	0.	1.700
3	191	14.476	14.476	1.108	0.	1.700
4	192	15.176	14.476	1.108	0.	1.700
5	193	16.476	16.476	1.108	0.	1.700
6	151	16.912	14.595	38.502	1943.746	1.700
7	151	16.912	14.595	38.502	1943.746	1.700
8	152	80.731	20.930	243.413	42726.324	1.701
9	153	82.835	21.507	245.733	39699.600	2.501
10	154	66.172	18.773	206.290	30540.937	2.502
11	155	63.487	16.305	194.756	21451.466	5.001
12	156	34.321	8.196	105.120	9766.540	12.200
13	157	24.340	5.515	81.158	6421.258	12.200
14	157	24.340	5.515	81.158	6421.258	12.200
15	158	4.588	2.797	19.617	-892.969	12.200
16	159	8.911	6.888	26.739	-1914.288	7.800
17	160	13.099	10.748	35.505	-2310.870	4.200
18	161	16.297	13.944	38.100	894.115	2.500
19	162	27.946	14.707	95.530	7275.440	2.500
20	163	29.131	15.402	99.315	8873.031	1.700
21	164	22.015	14.861	68.412	4493.193	1.700
22	164	22.015	14.861	68.412	4493.193	1.700
23	165	43.788	16.292	145.437	14871.125	1.704
24	166	43.084	16.184	144.799	15603.446	1.700
25	187	16.942	14.622	38.558	1946.327	1.700
26	187	16.942	14.622	38.558	1946.327	1.700
27	194	16.503	16.503	0.974	0.	1.700
28	195	14.503	14.503	0.974	0.	1.700
29	196	14.503	14.503	0.974	0.	1.700
30	186	14.503	14.503	0.974	0.	1.700

NASA National Aeronautics and Space Administration

Report Documentation Page

1. Report No.	2. Government Accession No.	3. Recipient's Catalog No.
CR - 189088		

4. Title and Subtitle

Component-Specific Modeling

5. Report Date
January 1992

6. Performing Organization Code

7. Author(s)

R. L. McKnight, R. J. Maffeo, M. T. Tipton, G. Weber

8. Performing Organization Report No.

9. Performing Organization Name and Address

General Electric Company
Aircraft Engine Business Group
Cincinnati, Ohio 45215

10. Work Unit No.
505-63-5B(AERO)

11. Contract or Grant No.
NAS 3-23687

12. Sponsoring Agency Name and Address

National Aeronautics and Space Administration
Lewis Research Center
Cleveland, Ohio 44135-3191

13. Type of Report and Period Covered
Final Report

14. Sponsoring Agency Code

15. Supplementary Notes

Project Manager, Christos C. Chamis, Structures Division, NASA Lewis Research Center, (216) 433-3252.

16. Abstract

Accomplishments are described for a 3-year program to develop methodology for component-specific modeling of aircraft engine hot section components (turbine blades, turbine vanes, and burner liners). These accomplishments include: (1) engine thermodynamic and mission models, (2) geometry model generators, (3) remeshing, (4) specialty 3-D inelastic structural analysis, (5) computationally efficient solvers, (6) adaptive solution strategies, (7) engine performance parameters/component response variables decomposition and synthesis, (8) integrated software architecture and development, and (9) validation cases for software developed.

17. Key Words (Suggested by Author(s))	18. Distribution Statement
Hot section components, analysis modeling, geometry generators, thermodynamic model, mission model, software architecture, decomposition, synthesis, adaptive solutions.	Unclassified-Unlimited Subject Category 39

19. Security Classif. (of this report)	20. Security Classif. (of this page)	21. No. of pages	22. Price
Unclassified	Unclassified	100	

NASA FORM 1626 OCT 86